nature plants

Article

https://doi.org/10.1038/s41477-025-02178-4

Rapid local and systemic jasmonate signalling drives the initiation and establishment of plant systemic immunity

Received: 16 May 2024

Accepted: 17 November 2025

Published online: 6 January 2026

Check for updates

Trupti Gaikwad[1,6,8], Susan Breen[1,7,8], Emily Breeze[1,8], Erin Stroud[1,8], Rana Hussain[1], Satish Kulasekaran[2], Nestoras Kargios[1], Fay Bennett[1], Marta de Torres-Zabala[3], David Horsell[4], Lorenzo Frigerio[1], Pradeep Kachroo[5] & Murray Grant[1]

Successful recognition of pathogen effectors by plant disease resistance proteins, or effector-triggered immunity (ETI), contains the invading pathogen through localized hypersensitive cell death. ETI also activates long-range signalling to establish broad-spectrum systemic acquired resistance (SAR). Here we describe a sensitive luciferase (LUC) reporter that captures the spatial–temporal dynamics of SAR signal generation, propagation and establishment in systemic responding leaves following ETI. *JASMONATE-INDUCED SYSTEMIC SIGNAL 1* (*JISS1*) encodes an endoplasmic-reticulum-localized protein of unknown function. *JISS1*::*LUC* captured very early ETI-elicited SAR signalling, which surprisingly was not affected by classical SAR mutants but was dependent on calcium and was also wound responsive. Both jasmonate biosynthesis and perception mutants abolished *JISS1*::*LUC* signalling and SAR to *Pseudomonas syringae*. Furthermore, we discovered that ETI initiated jasmonate-dependent systemic surface electrical potentials. These surface potentials were dependent on both glutamate receptors and JISS1, despite neither *JISS1* loss-of-function nor glutamate receptor mutants altering SAR to *Pseudomonas syringae*. We thus demonstrate that jasmonate signalling, usually associated with antagonism of defence against biotrophs, is crucial to the rapid initiation and establishment of SAR systemic defence responses (including the activation of systemic surface potentials) and that *JISS1*::*LUC* serves as a reporter to further dissect these pathways.

Despite the discovery of plant systemic acquired resistance (SAR) over a century ago, our knowledge of the signalling processes underlying the establishment, propagation and especially initiation of this response remains fragmentary. Classically, SAR is established following effector-triggered immunity (ETI) leading to the hypersensitive response (HR). SAR has also been reported to be activated via pathogen-associated molecular pattern recognition and virulent bacterial phytopathogens, although the latter has also been reported to trigger systemic induced susceptibility[1,2].

Multiple molecules are implicated in SAR induction, including salicylic acid (SA) and its volatile derivative methyl salicylate, azelaic acid (AZA), glycerol-3-phosphate, dehydroabietinal, pipecolic acid (Pip) and *N*-hydroxy-pipecolic acid (NHP). More recently, extracellular NAD(P), the volatile monoterpenes α- and β-pinene, vitamin B6 and small RNAs derived from *TAS3a* were shown to induce SAR[3–6]. HR-generated reactive oxygen species (ROS) and nitric oxide (NO) are integral to ETI-initiated SAR, most likely via C_{18} unsaturated fatty acid oxidation of chloroplast lipids[2,7]. Hydrolysis of C_{18} fatty acids released

A full list of affiliations appears at the end of the paper. e-mail: m.grant@warwick.ac.uk

from thylakoid membrane monogalactosyldiacylglycerol and digalactosyldiacylglycerol generates AZA[8,9]. The importance of lipid signalling in SAR is highlighted by the involvement of lipid transfer proteins, AZELAIC ACID INDUCED1 (AZI1) and DEFECTIVE IN INDUCED RESISTANCE1 (DIR1)[8]. Plants defective in SA, glycerol-3-phosphate, NO or ROS biosynthesis have reduced levels of Pip in distal tissues, reinforcing the complex metabolic interplay in the establishment of SAR[10]. Airborne defence cues also activate SAR[11]; thus, one can conclude that multiple signals translocating apoplastically, symplastically[12,13] and as volatiles can collectively confer broad-spectrum systemic resistance against diverse pathogens, including viral, bacterial, oomycete, fungal and insect pests[2]. The synthesis, activities and interactions of these SAR inducers have been extensively reviewed[10,14–16].

Despite progress in understanding the individual signalling networks leading to SAR, the spatial–temporal dynamics and interactions of various chemical signals in the SAR pathway remain unclear. Recognition of *Pseudomonas syringae* pv. *tomato* DC3000 (DC) carrying *avrRpm1* (DC*avrRpm1*)[17] by the Resistance to *P. maculicola 1* (RPM1) disease resistance protein provides a robust ETI model to dissect signal generation and transduction dynamics underlying SAR. We previously demonstrated that RPM1 activation triggers early increases in cytosolic calcium, beginning ~1.5–2 h post-infection (hpi)[18,19], followed by lipid-peroxidation-triggered biophoton generation ~3 hpi[20,21] and visible leaf collapse ~6 hpi. RPM1 activation elicits rapid transcriptional reprogramming 4 hpi in systemic leaves, which strongly overlaps with jasmonate-triggered systemic wound responses[22]. Here we report *JASMONATE-INDUCED SYSTEMIC SIGNAL 1* (*JISS1*), a jasmonate-responsive SAR reporter that captures unexpectedly rapid temporal–spatial dynamics following ETI. We show that SAR requires enzymatic production of a local jasmonate signal that propagates via the vasculature and epidermal cells to systemic leaves and is coupled to calcium- and jasmonate-dependent systemic surface electrical potentials.

Results

JISS1 expression reveals temporal and spatial dynamics of early effector–resistance gene interactions

JISS1 (At5g56980; previously known as A70 (ref. 22)), a protein of unknown function, is an early SAR marker[22]. To monitor SAR transcriptional dynamics, we fused the promoter of *JISS1* and the sequence encoding the first 84 amino acids of JISS1 to luciferase (Extended Data Fig. 1). Homozygous *JISS1* promoter::*luciferase* (*JISS1*::*LUC*) lines showed rapid systemic luciferase activity following challenge with DC*avrRpm1*, but not with virulent DC; the type-III-secretion-system-deficient DC*hrpA*, which elicits pathogen-associated-molecular-pattern-triggered immunity (PTI) responses; or mock challenge ($MgCl_2$) (Fig. 1a). SAR signal propagation was remarkably rapid, with strong luciferase activity first evident in the petiole of the challenged leaf ~3 hpi (Fig. 1b), and within 30 min *JISS1*::*LUC* activity was established[23,24]. This activity spread to adjacent leaves (~4 hpi, Fig. 1b), reaching maximal intensity ~4.5 hpi, ~1 h prior to any visible collapse of the challenged leaf.

Challenge with DC*avrRpt2* or DC*avrRps4* also induced systemic luciferase activity following recognition by Resistance to *P. syringae* 2 (RPS2)[25] and RPS4 (ref. 26), respectively (Fig. 1c). The spatial pattern of systemic luciferase reporter activity was identical for all ETI responses, but initiation timing differed for each resistance (R) protein, consistent with rapid translocation of an ETI-induced signal (Fig. 1c,d and Supplementary Video 1). To understand the temporal context of R protein elicitation, we investigated local ETI dynamics using two non-destructive physiological readouts, chlorophyll fluorescence and biophoton generation. The chloroplast senses and responds to biotic stress, best exemplified by decreases in the quantum efficiency of photosystem II (F_v/F_m) following ETI elicitation[27]. Quantitative and spatial F_v/F_m parameters were determined following challenge with DC*avrRpm1*, DC*avrRpt2*, DC*avrRps4* or the DC*hrpA* control (Fig. 1e,f and Extended Data Fig. 2a,b). Biophotons, generated from chloroplast lipid peroxidation[21] and associated with the initiation of the HR[20], were additionally assayed (Extended Data Fig. 2c and Supplementary Video 2). Systemic signal initiation elicited by these three R proteins is preceded in the local challenged leaf initially by strong suppression of F_v/F_m and subsequently by biophoton generation. Although DC*avrRpt2* challenge led to earlier suppression of F_v/F_m and biophoton generation than DC*avrRps4*, *JISS1*::*LUC* activation was faster following DC*avrRps4* challenge. These data imply that SAR signal generation is not definitively linked to biophoton generation and F_v/F_m suppression.

Jasmonates are involved in ETI-induced systemic signalling

To examine the regulation of *JISS1* in SAR, we crossed the *JISS1*::*LUC* reporter into classical SAR mutant lines expediated by identifying the *JISS1*::*LUC* transfer DNA (T-DNA) insertion position (Extended Data Fig. 1b): *npr1*, where *NONEXPRESSOR OF PATHOGENESIS-RELATED 1* (*NPR1*) encodes a repressor of ETI but is important for SAR[28–30]; *npr1 npr3 npr4* (ref. 28), impaired in SA signal transduction (notably, NPR3/4 is required for full RPS2 ETI)[31]; *nac19 nac55 nac72*, altered in the regulation of SA accumulation[32]; and *SA INDUCTION DEFICIENT 2* (*sid2*), deficient in the accumulation of SA[33]. Surprisingly, when challenged with DC*avrRpm1*, all SAR-compromised lines showed wild-type reporter dynamics (Fig. 2a and Extended Data Fig. 3a). Furthermore, SAR elicitors, AZA (or nonanoic acid (NA), its precursor), Pip and NHP did not significantly increase local JISS1–LUC activity (Fig. 2b), and JISS1–LUC activity in the NHP biosynthetic *FLAVIN-DEPENDENT MONOOXYGENASE 1* (*fmo1*) mutant[34] was wild-type-like in response to DC*avrRpm1* (Fig. 2c). Together, these data indicate that the signal inducing *JISS1* occurs upstream of or in parallel to previously characterized SAR elicitors.

We next tested key immunity-associated phytohormones for JISS1 induction. Even at high concentrations, leaves infiltrated with SA (1 mM) or abscisic acid (ABA; 1 mM) failed to elicit JISS1–LUC activity. However, jasmonic acid (JA; 250 µM), a key elicitor of systemic wound signalling, induced luciferase locally (Fig. 2d). Collectively, jasmonates comprise JA and its derivatives, with bioactive jasmonoyl-isoleucine (JA-Ile) binding the Skp/Cullin/F-box SCF^{COI1} (CORONATINE-INSENSITIVE PROTEIN 1)–JAZ1 E3 ubiquitin ligase jasmonate co-receptor complex[35,36]. DC does produce the highly active JA-Ile mimic coronatine (COR), but not until ~10 hpi[36,37]. Strikingly, 500 nM COR strongly induced JISS1–LUC locally within 2 h (relative to $MgCl_2$ or wounding; Fig. 2e and Extended Data Fig. 3b,c). JISS1–LUC was also induced in plants inoculated with both DC and the DC*cor*$^-$ mutant[38] bacteria expressing *avrRpm1* (Fig. 2f), excluding COR as the systemic elicitor.

ETI elicits a rapid and propagative jasmonate-dependent signal essential for effective SAR

We reported significant transcriptional overlap between the JA-regulated wounding response and the SAR response at 4 hpi with DC*avrRpm1* compared with mock challenges[22]. Re-examination of these data identified nine *JASMONATE ZIM DOMAIN* (*JAZ*) family members (including *JAZ10*), which act to reimpose the repression of jasmonate signalling[36,39], induced systemically by DC*avrRpm1* (Supplementary Table 2). As for JISS1, the wound-responsive JAZ10–GUS reporter[40] is also activated in systemic leaves challenged with DC*avrRpm1*, but not DC or DC*hrpA* (Fig. 3a). This systemic JAZ10–GUS expression is abolished in the jasmonate receptor mutant *coi1-16* (Fig. 3a)[41]. Following DC*avrRpm1* challenge, JISS1–LUC systemic expression was not detected in the JA biosynthetic mutant (*ALLENE OXIDE SYNTHASE*) (*aos*)[42] (Fig. 3b), and *JISS1* expression was reduced compared with that in Col-0 (Extended Data Fig. 4a). While local application of JA or COR to *JISS1*::*LUC coi1-16* failed to elicit local or systemic signals (Fig. 3c), it restored signalling in the *JISS1*::*LUC aos* plants (Fig. 3d).

We next determined whether the HR was impacted in *aos* or *coi1-16* mutants. Consistent with biophoton and chlorophyll fluorescence data, collapse of the wild-type Col-0 leaf occurred first with DC*avrRpm1*

https://doi.org/10.1038/s41477-025-02178-4

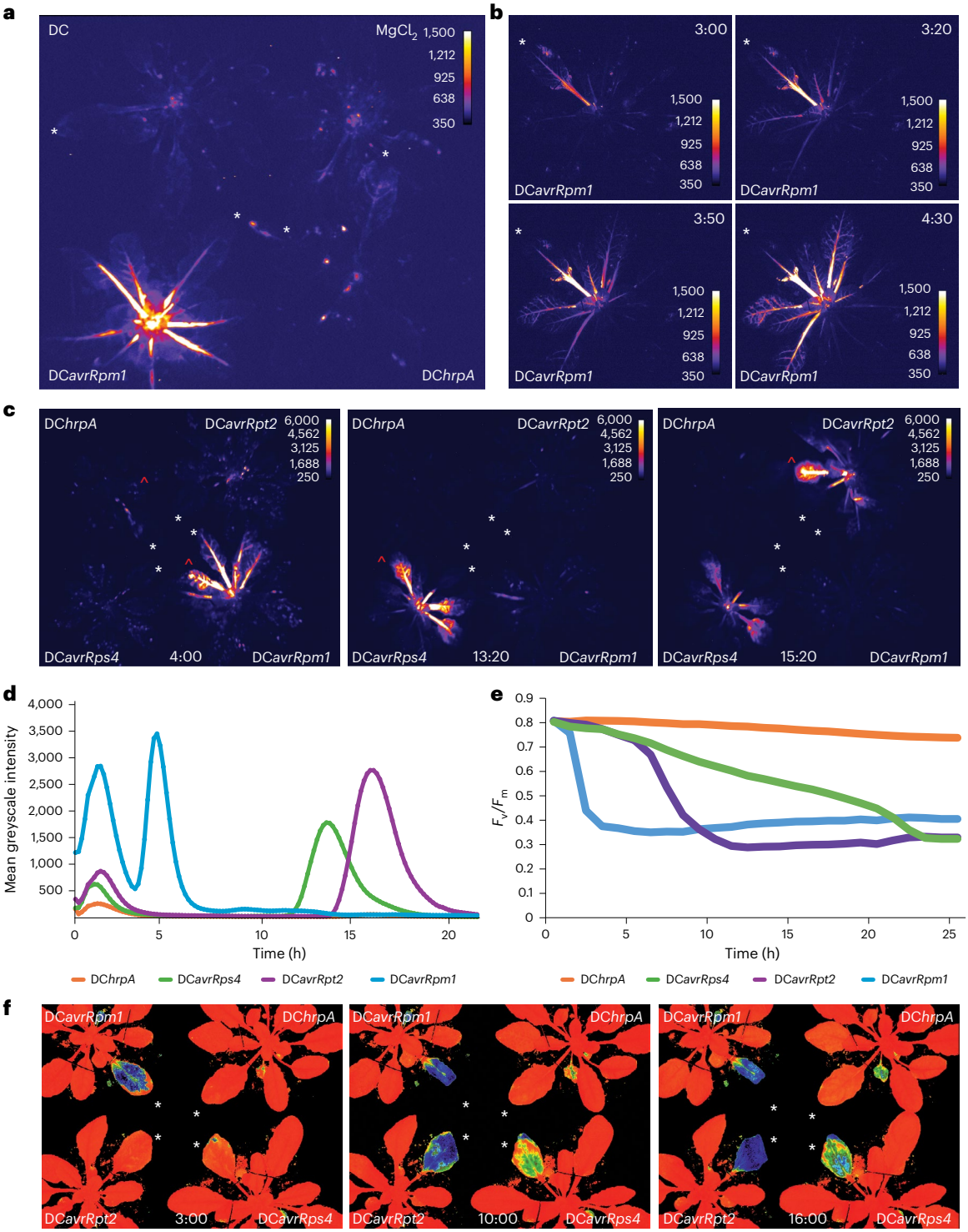

Fig. 1 | *JISS1* expression is induced systemically by ETI. a, Luciferase activity in *JISS1*::*LUC* plants following DC*avrRpm1*, DC, DC*hrpA* or mock ($MgCl_2$) challenges at 4:30 hpi. Throughout the figure, white asterisks indicate infiltrated leaves, and red carets indicate leaves used for signal intensity analysis (**d**). The images are false-coloured by signal intensity, as indicated by individual calibration bars. **b**, Temporal spatial dynamics of luciferase activity in *JISS1*::*LUC* plants following DC*avrRpm1* challenge, initiating at 3 hpi. The 3:20 hpi, 3:50 hpi and 4:30 hpi images capture the systemic spread of the signal over time. **c**, Different *Avr* genes display temporal specificity in the activation of systemic *JISS1*::*LUC*: DC*avrRpm1* (4 hpi), DC*avrRps4* (13:20 hpi) and DC*avrRpt2* (15:20 hpi), compared with the DC*hrpA* control. **d**, *JISS1*::*LUC* signal intensity in leaves adjacent to infiltration (red carets in **c**) plotted over time (h). **e**, F_v/F_m is strongly suppressed during ETI following DC*avrRpm1* (3 hpi), DC*avrRpt2* (10:00 hpi) or DC*avrRps4* (16:00 hpi) challenge compared with DC*hrpA*. **f**, Visualization of F_v/F_m suppression wherein orange indicates F_v/F_m of a healthy leaf (~0.8), green represents a reduction in F_v/F_m as ETI progresses (~0.6) and blue represents a strong impact of ETI on F_v/F_m (~0.3). Representative images of over ten repeats are shown.

https://doi.org/10.1038/s41477-025-02178-4

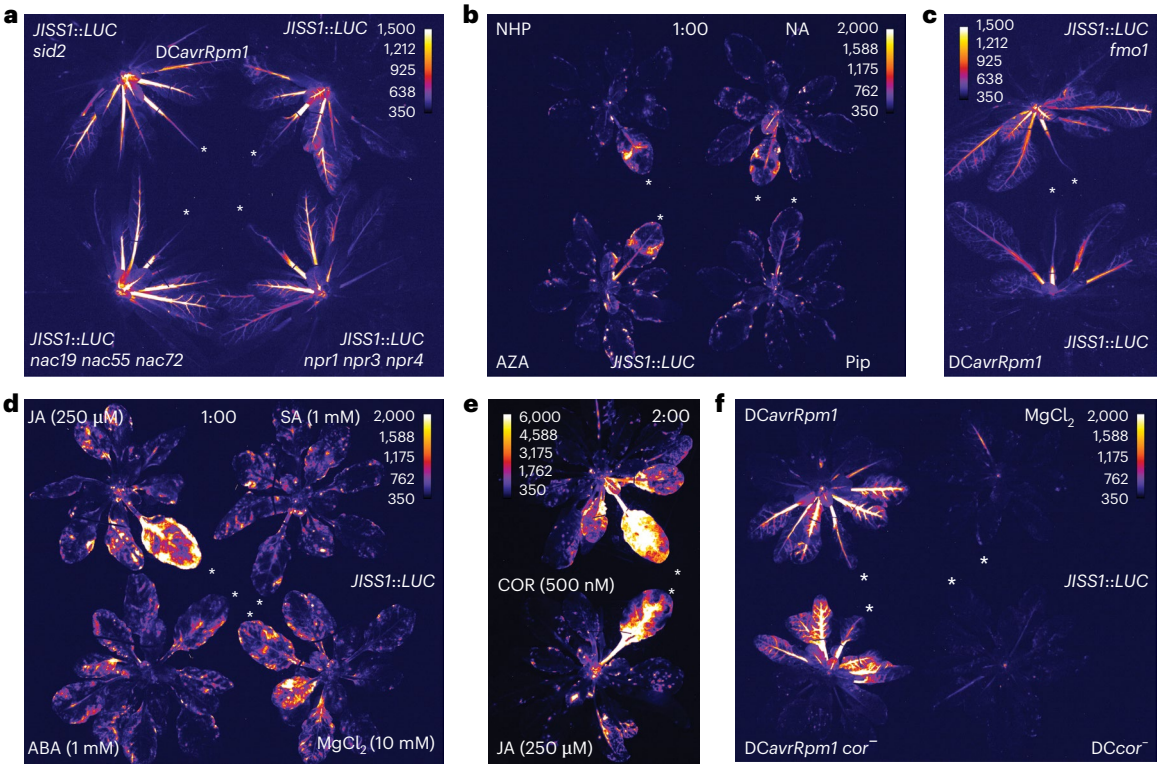

Fig. 2 | *JISS1*::*LUC* is activated by the jasmonate signalling pathway but not classical SAR elicitors. a, The classical SAR mutants *sid2*, *nac19 nac55 nac72* and *npr1 npr3 npr4* do not alter *JISS1*::*LUC* luciferase signatures following DC*avrRpm1* challenge (4 hpi). Throughout the figure, white asterisks indicate infiltrated leaves, and the images are false-coloured by signal intensity, as indicated by individual calibration bars. **b**, Infiltration of 1 mM Pip, NHP, NA or AZA into leaves of *JISS1*::*LUC* plants does not activate luciferase signal (1 hpi). **c**, No attenuation of luciferase activity is observed in a *JISS1*::*LUC fmo1* mutant line following DC*avrRpm1* challenge (4:30 hpi). **d**, JA (250 µM), but not SA (1 mM), ABA (1 mM) or mock (10 mM $MgCl_2$) challenge induces local *JISS1*::*LUC* signal propagation (1 hpi). **e**, Luciferase activity in *JISS1*::*LUC* leaves infiltrated with JA (250 µM) or COR (500 nM) (2 hpi). **f**, *JISS1*::*LUC* activity following challenge with DC or the COR-deficient DC mutant DB4G3 (*cor*$^-$) with or without *avrRpm1*. DC*avrRpm1 cor*$^-$ induced comparable *JISS1*::*LUC* systemic activity to DC*avrRpm1*, whereas no luciferase activity was detected in DC*cor*$^-$ challenged leaves (3:50 hpi). Representative images of at least three repeats are shown.

(~5.5 hpi), followed by DC*avrRpt2* (~14 hpi) and then DC*avrRps4* (~18 hpi). Crucially, timing of the HR was comparable between Col-0 and the *aos* and *coi1-16* mutants (Extended Data Fig. 4b), indicating that the loss of jasmonate biosynthesis or perception does not attenuate local HR but does attenuate JISS1–LUC local and systemic signalling and abolishes SAR. We thus concluded that systemic signalling is both jasmonate and HR dependent.

Aside from JA-Ile, other jasmonate molecules have biological activity in planta[43], including 12-oxophytodienoic acid (OPDA), although OPDA is not perceived by the SCF^{COI1} receptor complex[44]. We tested the JA biosynthetic inhibitors phenidone, a lipoxygenase inhibitor[45]; diethyldithiocarbamic acid (DIECA), which interferes with octadecanoid signalling[46]; and jarin-1, an inhibitor of JA-Ile synthetase[47] (Fig. 3e). Concurrent with DC*avrRpm1* challenge, treatment with phenidone (2 mM), DIECA (2.5 mM) or jarin (25 µM), via co-infiltration, petiole application or infiltration into the adjacent systemic responding leaves, abolished or markedly attenuated DC*avrRpm1*-elicited JISS1–LUC activity (Fig. 3f–i). These data independently reinforce a role for jasmonates in SAR, in both local signal generation and establishment in naive responding leaves, and specifically implicate JA-Ile biosynthesis as being necessary for both effective signal transduction and the establishment of SAR.

The *coi1* mutant is known to be more resistant to local DC challenge than wild-type *Arabidopsis*[41]. We assessed SAR to different *P. syringae* pathovars (less virulent *P. syringae* pv. *maculicola* race 4 (*Psm4*) or more virulent DC) in the *aos* and *coi1-16* mutants alongside a *JISS1* T-DNA insertion loss-of-function line (*jiss1*; Fig. 3j and Extended Data Figs. 4c and 5a,b). Crucially, neither *coi1-16* nor *aos* exhibited SAR relative to Col-0 across multiple independent assays ($n > 4$). Interestingly, *jiss1* lines still induced SAR following DC*avrRpm1* challenge (Fig. 3j and Extended Data Fig. 5c).

These data collectively imply that ETI elicits rapid de novo synthesis of a jasmonate-dependent signal that propagates systemically and is essential for the effective establishment of SAR. *JISS1* expression is intimately linked to this signal, but JISS1 itself is not critical for SAR or SAR signalling (Extended Data Fig. 5c–f), and its precise biological function remains unclear.

JISS1 signal localizes to the vasculature and epidermal endoplasmic reticulum

We next investigated JISS1 subcellular localization and expression following ETI elicitation. JISS1 was annotated as chloroplast localized (TAIR10; AtSubP). We thus generated both a full-length (*$JISS1_{pro}$*::*JISS1-GFP*) and a truncated JISS1–GFP fusion (*$JISS1_{pro}$*::*$JISS1^{1-84}$-GFP*); the latter included the predicted chloroplast transit peptide. In both lines, GFP signal was detected in the systemic leaf within 4.5 hpi, predominantly in both the vasculature and epidermal cells of the petiole and lamina (Fig. 4a,b and Extended Data Fig. 6a). Within the epidermal cells, both versions of the JISS1–GFP fusion proteins surprisingly localized to the endoplasmic reticulum (ER) network, colocalizing with the ER luminal marker, RFP–HDEL (Fig. 4c and Extended Data Fig. 6b). These data are suggestive of a SAR signal moving symplastically and are consistent with the abolition of SAR in plasmodesmata-permeability-restricted *Arabidopsis* overexpressing PLASMODESMATA-LOCATED PROTEIN 5 (ref. 13). As observed with JISS1–LUC activity, GFP expression in systemic leaves was markedly

https://doi.org/10.1038/s41477-025-02178-4

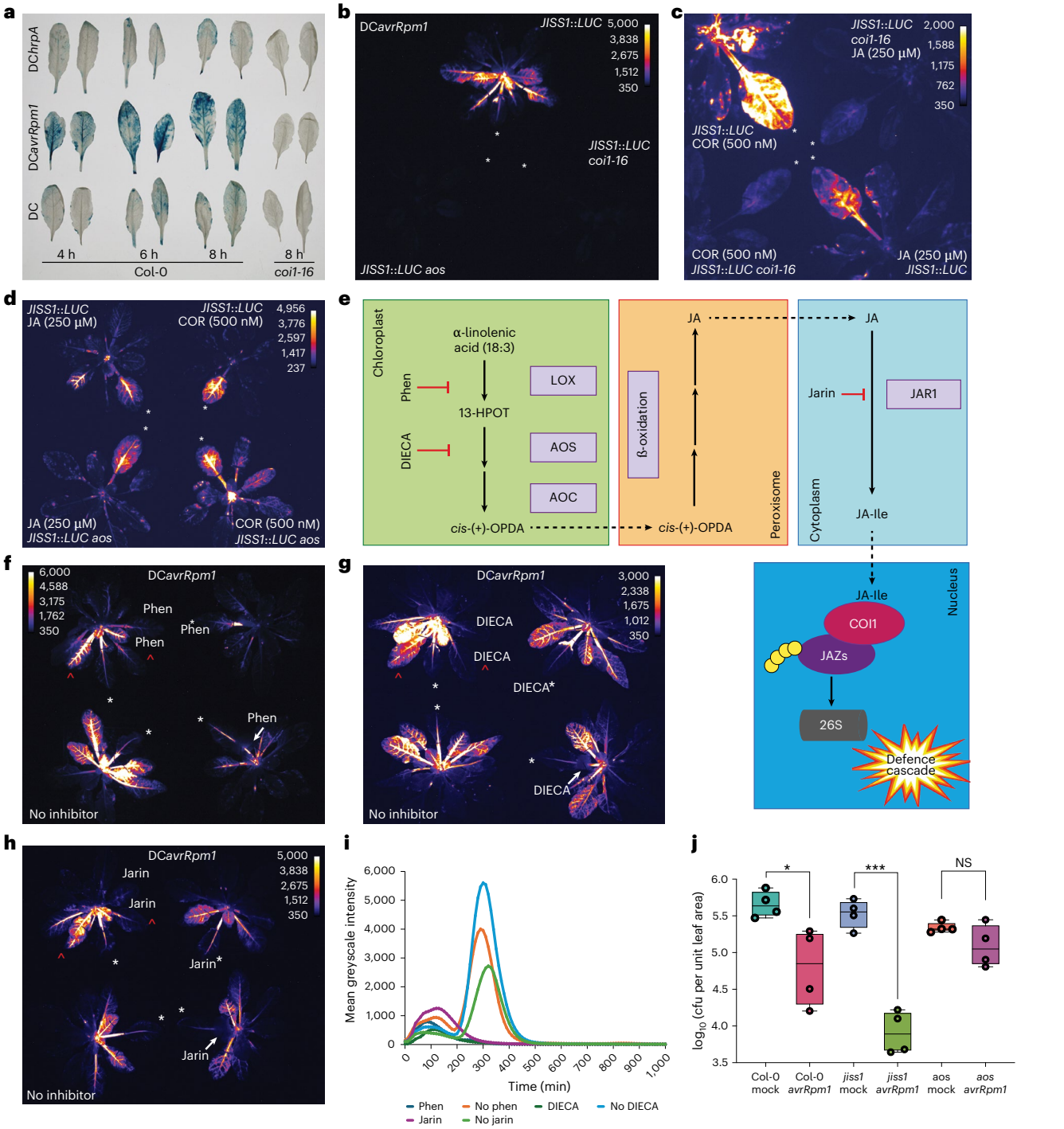

Fig. 3 | *JISS1*::*LUC* signal propagation is dependent on JA biosynthesis and perception. a, DC*avrRpm1* GUS activity in representative systemic leaves of a *JAZ10*::*GUS* reporter line at the times indicated compared to a *JAZ10*::*GUS coi1-16* line 8 hpi ($n = 4$ biological replicates). Throughout the figure, white asterisks indicate infiltrated leaves, and red carets indicate leaves used for signal intensity analysis. The images are false-coloured by signal intensity, as indicated by individual calibration bars. **b**, Luciferase activity is not induced in DC*avrRpm1*-treated *JISS1*::*LUC aos* or *JISS1*::*LUC coi1-16* mutant lines (5 hpi). **c**, Luciferase activity is absent in a *JISS1*::*LUC coi1-16* mutant but not *JISS1*::*LUC* leaves 1 hpi following infiltration with 250 µM JA or 500 nM COR (a JA-Ile mimic). **d**, Luciferase activity is restored in *JISS1*::*LUC aos* treated with 250 µM JA or 500 nM COR 1 hpi. **e**, Schematic of the JA biosynthetic pathway highlighting the positions of jasmonate inhibitor activity. 13-HPOT, 13-hydroperoxy-9,11,15-octadecatrienoic acid. **f**–**h**, Treatment with phenidone (Phen) (2 mM; 4:40 hpi) (**f**), DIECA (2.5 mM; 5:30 hpi) (**g**) or jarin-1 (25 µM; 5:10 hpi) (**h**) inhibits DC*avrRpm1*-induced *JISS1*::*LUC* activity. In **f**–**h**, the top left image shows the inhibitor pre-infiltrated into the right-hand systemic leaf immediately adjacent to the local challenged leaf, the top right image shows the challenged leaf co-infiltrated with the inhibitor, the bottom right image shows the petiole of the immunized leaf treated with the inhibitor and the bottom left image shows the leaves with no inhibitor. **i**, *JISS1*::*LUC* signal intensity in two leaves adjacent to DC*avrRpm1* infiltration, one treated with inhibitor and one without inhibitor (red carets in **f**–**h**) plotted over time (min). **j**, SAR growth curve of DC following DC*avrRpm1* or mock immunizing challenge on Col-0 (*$P = 0.0219$, $t = 3.068$, d.f. = 6 (unpaired two-tailed t-test)), *jiss1* (***$P < 0.0001$, $t = 9.162$, d.f. = 6) and *aos* (not significant (NS), $P = 0.1415$, $t = 1.692$, d.f. = 6). ($n = 4$ biological replicates). Box plots represent the minimum, maximum and median values for the statistical analysis of each treatment. Col-0 mock: min = 5.47, max = 5.88, median = 5.64, Q1 = 5.53, Q3 = 5.76; Col-0 DC*avrRpm1*: min = 4.20, max = 5.29, median = 4.85, Q1 = 4.43, Q3 = 5.22; *jiss1* mock: min = 5.26, max = 5.73, median = 5.55, Q1 = 5.45, Q3 = 5.63; *jiss1* DC*avrRpm1*: min = 3.64 max = 4.22, median = 3.89, Q1 = 3.67, Q3 = 4.13; *aos* mock: min = 5.28, max = 5.44, median = 5.32, Q1 = 5.31, Q3 = 5.35; *aos* DC*avrRpm1*: min = 4.81, max = 5.45, median = 5.05, Q1 = 4.88, Q3 = 5.26. The images are representative of at least three repeats.

https://doi.org/10.1038/s41477-025-02178-4

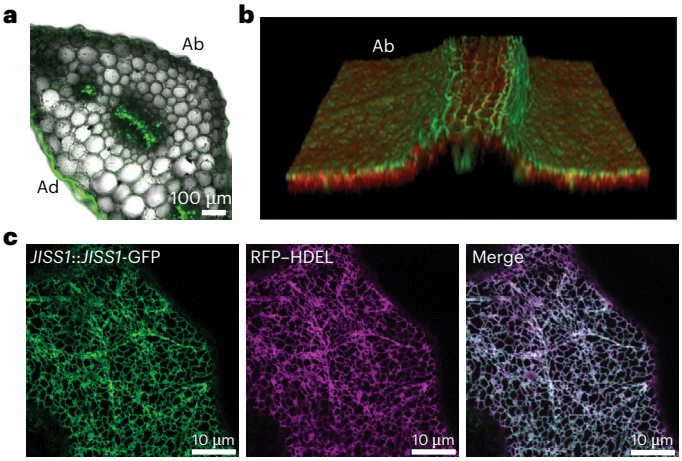

Fig. 4 | JISS1 signal propagates symplastically through the epidermis and vasculature and localizes to the ER. a–**c**, Confocal images of global *JISS1*::*JISS1-GFP* expression in representative systemic leaves following DC*avrRpm1* challenge. Panel **a** shows *JISS1*::*JISS1*$^{1–84}$*-GFP* expression in the petiole of a challenged leaf showing JISS1–GFP signal predominantly in the vasculature and epidermal cells. Ab, abaxial surface; Ad, adaxial surface. Scale bar, 100 µm. Panel **b** shows a still from Supplementary Video 3 of JISS1(1–84)–GFP highlighting that the GFP signal is predominately restricted to the central vasculature and abaxial epidermal cell layer. Panel **c** shows representative confocal images of *Arabidopsis* epidermal leaf cells stably expressing *JISS1*::*JISS1-GFP* (green) and the ER luminal marker RFP–HDEL (magenta), which shows that JISS1 localizes strictly to the ER. Scale bars, 10 µm. The images are representative of at least three biological replicates.

suppressed by pretreatment with the JA biosynthetic inhibitors phenidone and DIECA (Extended Data Fig. 6c).

Systemic electric signal propagation is a general feature of ETI activation

Wound-induced accumulation of JA and JA-Ile in undamaged distal leaves, together with altered expression of jasmonate-responsive genes, is preceded by the rapid generation of wound-activated surface electrical potentials (WASPs), caused by plasma membrane depolarization[40]. WASPs are mediated by glutamate-triggered systemic activation of cytosolic Ca^{2+} signalling via specific vasculature-localized members of the glutamate-like receptor family, GLR3.3 and GLR3.6 (refs. 40,48). These cation-permeable ion channels also contribute to systemic defence against herbivory[48]. To confirm the link between *JISS1* and JA signalling, we assayed the activity of *JISS1*::*LUC* in response to wound stimuli. Either crushing with forceps or severing the leaf at the petiole triggered rapid, transient induction of *JISS1*::*LUC* (Fig. 5a). Wounding induced a much weaker signal than COR application (Extended Data Fig. 3b,c). Given the similar spatial distribution of WASPs and JISS1–LUC signals, and the transcriptional parallels between wounding and early SAR responses[22], we measured leaf surface potentials between electrodes attached to the midrib/petiole junction of a local challenged leaf ('infiltrated') and to fully expanded leaves immediately adjacent to ('adjacent') and directly opposite ('distal') the challenged leaf (Fig. 5b).

No specific changes in leaf surface potentials were induced in untreated or DC*hrpA*-challenged leaves, whereas DC induced a small depolarization of the local challenged leaf (Fig. 5c and Extended Data Fig. 7a,b). By contrast, challenge with DC*avrRpm1* initially induced strong depolarization with an amplitude of about −100 mV over a duration of ~2 h, followed by repolarization (Fig. 5c and Extended Data Fig. 7c). The timing of depolarization strongly correlated with biophoton generation, the suppression of F_v/F_m and JISS1–LUC systemic signal initiation (Fig. 1 and Extended Data Fig. 2). Following repolarization of the challenged leaf, systemic immunity surface potentials (SISPs) were detected in adjacent leaves with maximal depolarization ~7 hpi. SISPs were also detected in distal leaves, but maximal depolarization occurred later (~10 hpi; Fig. 5c and Extended Data Fig. 7c). These SISPs, unlike WASPs and herbivory responses, which travel at speeds in excess of millimetres per second[49], represented slower variation potentials, which largely mirrored the spatial dynamics of systemic JISS1–LUC activity, albeit with delayed propagation. As both DC*avrRpt2* and DC*avrRps4* also trigger SISPs (Extended Data Fig. 7d,e) with the timing of initiation largely consistent with the initiation of suppression of F_v/F_m (Fig. 1e,f, and Extended Data Fig. 2a,b), we concluded that SISPs are specifically elicited by ETI.

Consistent with jasmonate dependency, SISPs were abolished in *coi1-16*, with only the DC*avrRpm1*-challenged leaf (red trace) undergoing initial depolarization (Fig. 5c and Extended Data Fig. 7f) Surprisingly, despite eliciting a local visible HR, SISPs were not induced by conditional (dexamethasone (Dex)) induction of *avrRpm1*. Instead, a steady depolarization of the induced leaf with no subsequent repolarization was observed (Fig. 5d and Extended Data Fig. 7g). However, co-infiltration of Dex-induced leaves with DC*hrpA* or DC (Fig. 5d and Extended Data Fig. 7h,i) broadly recapitulated SISP changes, implying that PTI is required for SISP generation.

We also measured SISPs in *glr3.3a*, *glr3.6a*, *jiss1* and the *glr3.3a glr3.6a* mutant, the latter of whose functions are necessary for full wound and herbivory responses[40,50]. Mirroring WASP attenuation[40], SISPs were abolished in the *glr3.3a*, *glr3.6a* and *glr3.3a glr3.6a* mutants (Fig. 6a and Extended Data Fig. 8a–c). *glr3.6a* showed depolarization of the local challenged leaf (Fig. 6a and Extended Data Fig. 8b)[50], which mirrored *jiss1* and *coi1-16* responses in which SISPs were abolished and depolarization was only seen in the local challenged leaf (Figs. 5c and 6a and Extended Data Figs. 7f and 8d).

Calcium signalling is necessary for systemic immunity

Given the finding that ETI alone is not sufficient to induce SISPs, we crossed *JISS1*::*LUC* into the *glr3.3a*, *glr3.6a* and *glr3.3a glr3.6a* mutants. Interestingly, JISS1–LUC dynamics were unaltered in all loss-of-function *glr* lines tested (Fig. 6b), though both *jiss1* and *glr* mutants lost the ability to generate SISPs.

AvrRpm1–RPM1 mediated SISP generation thus requires functional JISS1, COI1 and vasculature-specific GLR Ca^{2+} channels, which link systemic electrical signal propagation in response to wounding[40] and herbivory[50]. As the loss of GLRs does not abolish JISS1–LUC activity or SAR to *Psm4* (Fig. 6c), SISPs most likely encode another SAR signal, for example for herbivory responses. Since SISPs, like WASPs, are dependent on GLR3.3, which triggers long-distance calcium signalling[51], we investigated the role of calcium in JISS1–LUC activity. The calcium channel blocker $LaCl_3$ (1 mM) abolished DC*avrRpm1*-induced JISS1–LUC activity in systemic leaves, as did co-infiltration of $LaCl_3$ with DC*avrRpm1*. Also, the application of $LaCl_3$ to the petiole surface markedly attenuated JISS1–LUC activity (Fig. 6d). Therefore, Ca^{2+} signalling, which is intimately linked to ETI[52], is necessary for JISS1–LUC SAR activity and SISP propagation.

Discussion

SAR confers broad-spectrum resistance to viral, fungal, oomycete and bacterial pathogens and insect pests despite their diverse lifestyles and virulence strategies. A variety of signalling molecules have been shown to be important for SAR. Many of these are synthesized de novo, implying upstream inductive signals. Our current understanding of signal generation, translocation and establishment in systemic responding leaves is constrained by a lack of information on the spatial–temporal dynamics of SAR activation. Here we used *JISS1* (previously *A70*)[22], a jasmonate-responsive gene, to develop a reporter that overcomes these constraints to faithfully report ETI-elicited SAR. Using a *JISS1*::*LUC* reporter, chlorophyll fluorescence[27,53] and biophoton[20] imaging, we characterized SAR dynamics during HR elicited by

https://doi.org/10.1038/s41477-025-02178-4

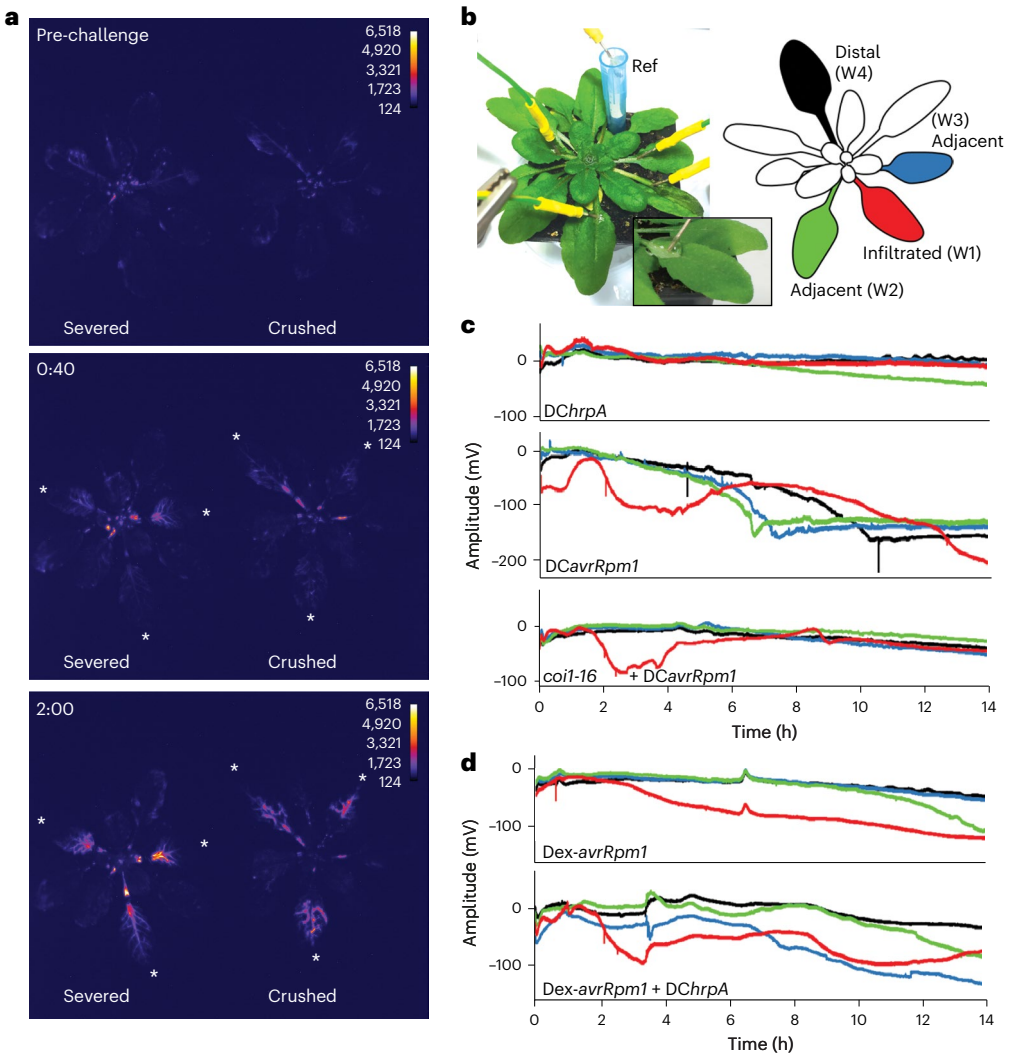

Fig. 5 | Systemic electric signal propagation is a general feature of ETI activation. a, White asterisks indicate wounded *JISS1*::*LUC* leaves, and the images are false-coloured by signal intensity, as indicated by individual calibration bars. Luciferase activity in severed or crushed leaves ($n = 3$) initiated and peaked at ~40 min and ~2 h post-wounding, respectively. **b**, Plant electrophysiology experimental set-up with a cartoon showing spatial sampling and colour coding of leaves for working electrodes (W). The inset illustrates electrode positioning. Ref, reference electrode. **c**, Leaves challenged by DC*avrRpm1* but not DC*hrpA* (red) show an initial depolarization ~2 hpi and subsequent repolarization. From 4 to 7 hpi, SISPs are propagated in the two systemic leaves (blue and green) adjacent to the DC*avrRpm1*-immunized leaf, with the distal leaf (black) responding later (from ~7 hpi). No SISPs are observed in the DC*hrpA* treatments. The *coi1-16* mutant shows depolarization of the DC*avrRpm1*-challenged leaf but no SISP initiation. **d**, Dex-induced *avrRpm1* expression does not replicate DC*avrRpm1*-induced SISPs; however, infiltration of DC*hrpA* 1 h after Dex application re-instigates SISPs. The experiments were repeated at least twice (see Extended Data Fig. 7 for further details).

two coiled-coil nucleotide-binding leucine-rich repeats (CNLs,RPM1 and RPS2) and a Toll-like/Interleukin 1 nucleotide-binding leucine-rich repeat receptor (TNL,RPS4). We demonstrate that jasmonate signalling is essential for SAR and further show that the ER-localized JISS1 is essential for the generation of electrical surface potentials in systemic responding leaves (SISPs), like those reported to underpin resistance to herbivory[50].

JISS1::*LUC* signal generation was unaffected in the mutants *sid2*, *npr1 npr3 npr4*, *fmo1* and *nac19 nac55 nac72* (Fig. 2 and Extended Data Fig. 3a). Infiltration of the SAR inducers NA, AZA, Pip and NHP also failed to induce *JISS1*::*LUC*. Of the classic plant immunity-associated hormones, neither ABA nor, unexpectedly, SA activated *JISS1*::*LUC*. JA and COR elicited local but not systemic luciferase activity, and COR-deficient DC*avrRpm1* still replicated *JISS1*::*LUC* temporal and spatial activation dynamics (Fig. 2).

Consistent with a key role for jasmonates in establishing SAR, both jasmonate biosynthetic (*aos*) and signalling (*coi1-16*) mutants were SAR deficient and failed to activate JISS1–LUC following DC*avrRpm1* challenge (Fig. 3b). These data expand our previous results[22] demonstrating compromised SAR in the JA biosynthetic mutant *opr3* (*12-OXOPHYTODIENOATE REDUCTASE 3*) and the JA signalling mutant *jin1* (*JASMONATE-INSENSITIVE 1*; *myc2*)[22]. Neither COR nor JA infiltration activated luciferase in *coi1-16 JISS1*::*LUC* plants (Fig. 3c), but their exogenous application restored activity in *JISS1*::*LUC aos* (Fig. 3d). Reinforcing the importance of jasmonate signalling, the JA-Ile synthetase inhibitor jarin (like phenidione and DIECA) significantly attenuated *JISS1*::*LUC* signal generation, propagation and distal activation (Fig. 3f–i). Interestingly, *jiss1* was SAR competent, and *jiss1 JISS1*::*LUC* lines were activated by ETI, indicative of a mobile jasmonate-dependent SAR signal propagating through the systemic tissue (Fig. 3j and Extended Data Fig. 5c–g). Thus, genetically, pharmacologically and spatially, via real-time transcription monitoring, we conclusively show a key role for jasmonates in SAR, independent of the classical SAR mutant lines *npr1*, *sid2*, *npr1 npr3 npr4* and *nac19 nac55 nac72*.

https://doi.org/10.1038/s41477-025-02178-4

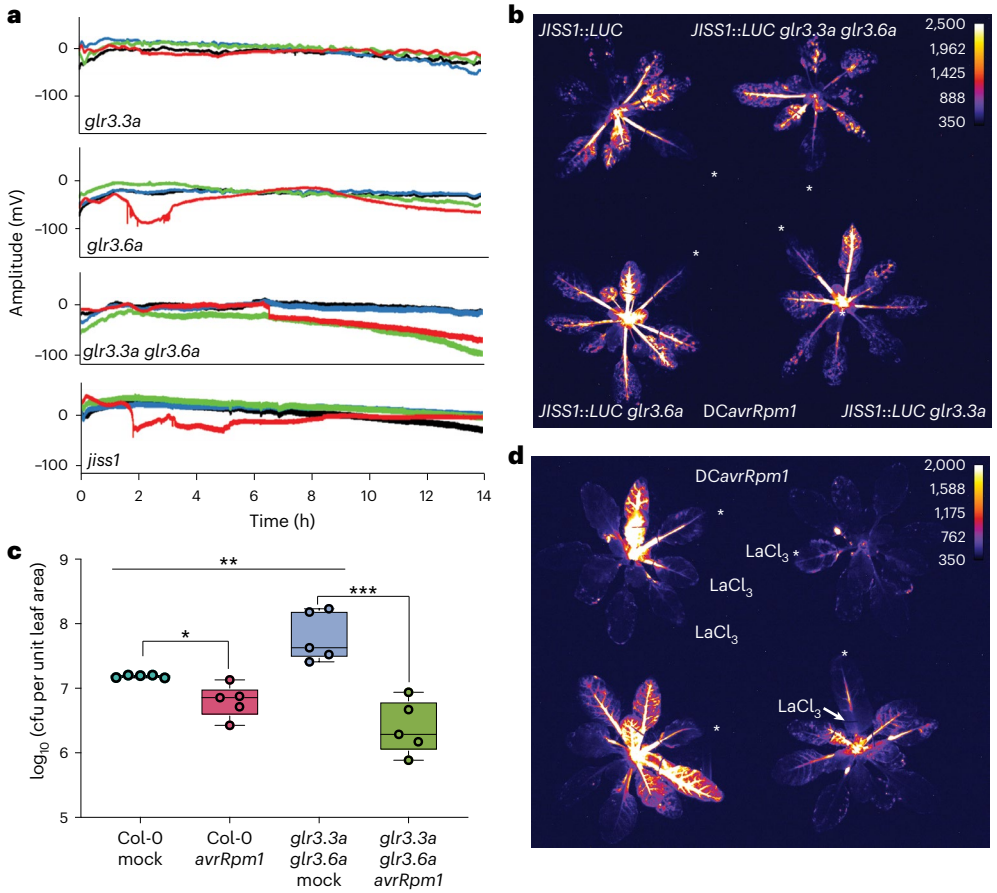

Fig. 6 | JISS1 systemic signal is calcium dependent. a, Glutamate receptor mutants *glr3.3a*, *glr3.6a* and *glr3.3a glr3.6a* do not propagate SISPs following DC*avrRpm1* challenge. *glr3.6a*, like *jiss1*, shows limited depolarization of the DC*avrRpm1*-challenged leaf. **b**, DC*avrRpm1*-challenged *JISS1*::*LUC glr3.3a glr3.6a*, *JISS1*::*LUC glr3.3a* and *JISS1*::*LUC glr3.6a* mutants all exhibited comparable systemic luciferase activity to that of *JISS1*::*LUC* (4:10 hpi). In **b** and **d**, white asterisks indicate infiltrated leaves, and luciferase images are false-coloured by signal intensity, as indicated by the calibration bars. **c**, SAR growth curve of *Psm4* following DC*avrRpm1* or mock pretreatment on Col-0 (*$P = 0.0102$, $t = 3.343$, d.f. = 8 (unpaired two-tailed t-test)) and the *glr3.3a glr3.6a* mutant (***$P = 0.0005$, $t = 5.550$, d.f. = 8). *glr3.3a glr3.6* mutant mock and the Col-0 mock were significantly different (**$P = 0.0076$, $t = 3.593$, d.f. = 8) ($n = 5$ biological replicates). Box plots represent the minimum, maximum and median values for the statistical analysis of each treatment. Col-0 mock: min = 7.16, max = 7.20, median = 7.19, Q1 = 7.17, Q3 = 7.20; Col-0 DC*avrRpm1*: min = 6.43, max = 7.13, median = 6.86, Q1 = 6.71, Q3 = 6.88; *glr3.3a glr3.6a* mock: min = 7.41, max = 8.23, median = 7.63, Q1 = 7.52, Q3 = 8.18; *glr3.3a glr3.6a* DC*avrRpm1*: min = 5.88, max = 6.94, median = 6.29, Q1 = 6.17, Q3 = 6.67. **d**, Treatment with the calcium inhibitor $LaCl_3$ (1 mM) inhibits DC*avrRpm1*-induced *JISS1*::*LUC* activity compared with the control (4:50 hpi). Top left, two systemic leaves below the challenged leaf were pre-infiltrated with $LaCl_3$. Top right, local leaf co-infiltrated with $LaCl_3$ and DC*avrRpm1*. Bottom right, petiole of an immunized leaf treated with $LaCl_3$. Bottom left, no inhibitor. All experiments were repeated at least three times with similar results. SAR (**c**) was evident with either DC and *Psm4* challenge or secondary challenges.

It may seem counterintuitive that jasmonates underpin SAR, given well-documented JA/SA antagonism in biotrophic immunity; however, SA/JA synergism has been reported[54]. Spatial separation of JA and SA signalling during ETI would be a parsimonious explanation for SA/JA dependency and reinforce the importance of short-distance local cellular signalling in ETI responses[55]. Indeed, dual-expressed SA and JA reporters exhibit temporally separated distinct concentric domains (inner/early for SA and outer/later for JA) between the ETI-responding cells[56], elegantly explaining the COI1 dependency of the *JISS1* reporter and the need to consider spatial cellular context during ETI signalling.

Our data support the model that early ETI leads to chloroplast ROS generation, indicative of the strong suppression of F_v/F_m[27] and subsequent biophoton generation[20,21]. Enzymatic and non-enzymatic chloroplast galactolipid-derived oxylipins[57,58] are thus potential substrates for the generation of jasmonate-based mobile SAR signals and JISS1–LUC activation. Both fatty acid desaturase and chloroplast galactolipid mutants necessary for JA synthesis are SAR deficient[7,9], whereas JA levels increase ~75-fold within 5–10 hpi of DC*avrRpm1* challenge[57].

The *JISS1* reporter also responded to wounding stimuli, consistent with our previous microarray data[22]. The spatial expression pattern of JISS1–LUC activity mirrored jasmonate-dependent WASPs[40]. ETI-responding leaves triggered surface depolarizations (~100 mV) comparable to WASPs, but SISP generation and propagation dynamics were markedly slower. Conditional expression of *avrRpm1* in planta was insufficient to generate SISPs and required pathogen-associated molecular patterns (Fig. 5d and Extended Data Fig. 7d). Interestingly, wounding and herbivory release damage-associated molecular pattern molecules[59,60]. Our results suggest that PTI/ETI mutual potentiation[61] may extend to SISP signalling.

Glutamate receptor-like mutants abolish WASPs[40,48] and were required for SISP generation. They have previously been implicated in PTI[62], resistance to pathogens[63] and anti-herbivory defence[50,51]. *glr3.3a* exhibited markedly less depolarization of the challenged leaf (Fig. 6a, red trace) than *glr3.6a*. Notably, *jiss1* failed to induce SISPs; also, like *jiss1*, no tested *glr* mutants abolished ETI *JISS1*::*LUC* activity, and *glr3.3 glr3.6* maintained SAR to *Psm4* (Fig. 6). Collectively, the loss of SISPs in *coi1-16* and *jiss1* (Figs. 5c and 6a) supports an additional role

for jasmonates and JISS1 in SISP generation. SISPs may thus represent one of a suite of signals that collectively drive reprogramming of distal leaves to confer broad-spectrum resistance. Indeed, we previously showed that the generalist insect *Helicoverpa armigera* modified its feeding behaviour on *Arabidopsis* leaves, moving away from regions where *JISS1*::*LUC* was induced[64].

Unlike JISS1, GLRs are believed to be ligand-gated channels. It remains unclear how either is activated to induce or maintain SISPs. More research is therefore necessary to understand the GLR mechanism of action in SISP generation. Localization of *JISS1*::JISS1–GFP predominantly to the epidermal ER and vasculature was unexpected. It is notable that both GLR3.3a and GLR3.6a localize to the leaf vasculature. Interestingly, GLR3.3a is primarily ER localized in phloem sieve elements, whereas GLR3.6a was predominantly in xylem contact cell tonoplast membranes[49,65]. Since distinguishing vascular cell types by cross-section is challenging, we examined single-cell transcriptomics data focusing on the vasculature[66] and cell layers on the adaxial leaf surface[67]. The majority of *JISS1* vascular expression was in a discrete xylem parenchyma cluster, which also showed strong representation of genes encoding hormone pathways including JA as well as specific amino acid biosynthetic and degradation pathways[66]. *JISS1* expression was also evident in bundle sheath, adaxial procambium stem cells and a phloem parenchyma cluster, whereas epidermal and guard cell *JISS1* expression was seen in general cell-type clusters. Procko et al.[68] identified *JISS1* in only 2 of 16 clusters corresponding to epidermal pavement and mesophyll/photosynthesis-related genes, both highly enriched for plant immune response transcripts.

In summary, *JISS1* encodes an ER-localized protein. The *JISS1* promoter functions as a dynamic spatial transcriptional SAR reporter, capturing propagative jasmonate-dependent signals rapidly moving through the vasculature, and symplastically via epidermal cells to systemic responding leaves. Our study reveals remarkable parallels between systemic wound signalling and the elicitation of SAR. Vascular jasmonate synthesis, such as in wounding, is well documented and has been attributed to electrical-signal-dependent remodelling of primary vein chloroplast galactolipids[65]. Here, *coi1*, *glr3.3a glr3.6a* and *jiss1* mutants all abolished SISPs, but the *glr* mutants (like *jiss1*) showed wild-type systemic JISS1–LUC signalling. This may represent an example of an amplification loop, considered widespread in systemic signalling[66]. Whereas ETI-mediated rapid jasmonate induction establishes defence against biotrophs, SISPs may propagate mobile information decoded systemically for anti-herbivory responses[50,51]. This study lays the foundation, and provides spatial–temporal tools, for dissecting the complex molecular mechanisms underpinning long-distance immune signalling.

Methods

Arabidopsis growth conditions

Arabidopsis thaliana were grown for four to five weeks in compost (Levingtons F2) in a controlled-environment growth chamber programmed at 60% relative humidity with 10 h days (21 °C; 120 µmol m^{-2} s^{-1}) and 14 h nights (21 °C) as previously described[37,67].

Generating *Arabidopsis* transgenic lines

The *JISS1*::*LUC* plants were generated as previously described[64]. In brief, the *Photinus pyralis LUC2P* reporter gene containing the hPEST protein destabilization sequence (Promega pGL4.11) was cloned into pCAMBIA1302 via the Kpn1 and Pml1 restriction sites, creating pC1LUCP. A 1,631-bp promoter fragment of *JISS1* was PCR amplified from Col-0 genomic DNA and cloned into pC1LUCP using the primers detailed in Supplementary Table 2. Transgenic homozygous *JISS1*::*LUC* lines were generated in the Col-5 background via floral dipping[69]. Ten lines were screened via DC*avrRpm1* challenge, and the genomic location of *JISS1*::*LUC* in the strongest-expressing line was identified within At4g39240 using adapter ligation-based PCR[70].

Subsequently, *JISS1*::*LUC* crosses into mutant plants were determined as homozygous via diagnostic PCR for *JISS1*::*LUC* insertion using the primers detailed in Supplementary Table 2. All other primers for validating mutants following crossing are shown in Supplementary Table 3. All homozygous *JISS1*::*LUC* mutant crosses were generated in the mutant parental Col-0 background.

The *JISS1*$^{1–84}$*-GFP* line was generated using restriction enzyme cloning. The *JISS1* promoter and initial coding sequence were amplified from genomic DNA using the primers detailed in Supplementary Table 2. The PCR product was cloned into pCAMBIA1305 as a carboxy-terminal fusion with GFP. The *JISS1* promoter full-length *JISS1*::*GFP* line was generated using the Golden Gate assembly system[71] as follows: the *JISS1* promoter was amplified as above and cloned into the level 0 plasmid pICH41295, while the full-length *JISS1* coding sequence was cloned into pAGM41287. The *JISS1* promoter and coding sequence were combined in the FL1P1 level 1 vector to create *JISS1*$_{pro}$::*JISS1-GFP*::*Ocs*. Finally, the level 2 vector FL1P2 with BASTA selection was used to allow selection in planta after transformation into the Col-0 background via standard methods.

The homozygous *JISS1*$_{pro}$::*JISS1-GFP* line was subsequently crossed with an *RFP-HDEL* (ER luminal marker) line (a gift from the late C. Hawes, Oxford Brookes University, UK).

The *JAZ10*::*GUS* line was a gift from E. Farmer (University of Lausanne), and the *npr1*, *npr1 npr3 npr4* and *nac19 nac55 nac72* mutants were a gift from X. Dong (Duke University). All other loss-of-function mutants and the Dex-*avrRpm1* line were obtained from the Nottingham *Arabidopsis* Stock Centre.

Bacterial growth, maintenance and inoculation

Bacterial cultures (*P. syringae* pv. *tomato* strains DC containing the empty cloning vector (pVSP61), DC*hrpA* and DC containing the avirulence gene *avrRpm1*, *avrRps4* or *avrRpt2*) were grown in Kings B medium[72] overnight with shaking (200 rpm) at 28 °C. Cells were harvested (2,000 *g* for 8 min), washed and resuspended in 10 mM $MgCl_2$ (ref. 67). *avrRpm1* (in pVSP61) was introduced into the DC COR-deficient mutant DB4G3 (*cor*$^{-1}$/*cor*$^{-2}$)[38]. For luciferase, GUS, phenotyping and GFP assays, selected leaves were inoculated with a 1-ml needleless syringe on their abaxial surface with the appropriate bacterial suspension adjusted to a final optical density at 600 nm (OD_{600}) of 0.15 in 10 mM $MgCl_2$ (or as otherwise indicated in the figure legends).

For SAR growth assays, the immunizing inoculation comprised either 10 mM $MgCl_2$ (mock) or OD_{600} 0.005 DC*avrRpm1*. Two days later, either *Psm4* or DC (see the figure legends) was inoculated at OD_{600} 0.001 or OD_{600} 0.002, respectively, using a similar protocol to ref. 73. Three days after DC or four days after *Psm4* challenges, bacterial growth measurements were determined from three inoculated leaves per plant and a minimum of four independent replicates. Significant growth differences between treatments were determined using Student's *t*-test (unpaired two-tailed). All experiments were repeated at least three times.

Chlorophyll fluorescence

Photosystem II chlorophyll fluorescence imaging of challenged leaves was performed with CF Imager software V2.305 (Technologica Ltd). Plants were placed in the chamber for 40 min post-inoculation and then dark adapted for 20 min. This was followed by a saturating light pulse (6,349 µmol m^{-2} s^{-1} for 0.8 s) to obtain maximum dark-adapted fluorescence (F_m). Actinic light (120 µmol m^{-2} s^{-1}) was then applied for 15 min, followed by a saturating pulse to obtain maximum light adapted fluorescence (F_m'). The plants remained in actinic light for a further 24 min and were then returned to a dark period of 20 min. This cycle (59 min long) was repeated 23 times. F_m, F_m' and F_o (minimal fluorescence with fully oxidized PSII centres) were used to calculate chlorophyll fluorescence parameters related to photosystem II: F_v/F_m (maximum dark-adapted quantum efficiency) and non-photochemical quenching. Data were extracted using CF Imager software V2.305 (Technologica Ltd).

Luciferase visualization
A solution of 1 mM luciferin (Promega) in 0.02% Silwet L77 (Loveland Industries, Ltd) was sprayed onto *JISS1*::*LUC* plants. The plants were kept in the dark for 30 min prior to inoculation. The petioles of the treated and adjacent rosette leaves were secured by folded paperclips to minimize epinastic movement. The plants were placed in a dark box, and images were captured using either an ORCAII ER CCD camera (Hamamatus Photonics) with a 35-mm f2.8 micro Nikkor lens or a Retiga R6 Scientific CCD camera (Qimaging) fitted with a Schneider STD XENON 25-mm lens. Photons were counted for 10 min at 2 × 2 binning mode, and data were acquired with either Wasabi (Hamamatsu) or Micro-Manager v.1.4 (Qimaging) software.

Biophoton visualization
Pathogen-challenged plants were placed inside a dark box mounted with a Retiga R6 camera with a 25-mm f1.4 Navitar lens. Digital monochrome images captured photons for 20 min at 2 × 2 binning mode using MicroManager v.1.4. False-colouring, brightness adjusting and annotation were performed using Fiji (ImageJ2 v.2.9.0/1.53t)[74], as described previously[20].

Chemicals
JA, SA, ABA, AZA, NA, Pip, DIECA, phenidone (1-phenyl-3-pyrazolidinone), lanthanum (III) chloride ($LaCl_3$) and COR were all from Sigma. NHP was synthesized by Accel Pharmtech, and jarin-1 was sourced from AOBIOUS Inc. All chemicals were used at the concentrations described in the figures. DIECA (2.5 mM), phenidone (2 mM), jarin-1 (25 µM) or $LaCl_3$ (1 mM) was pre-infiltrated into systemic leaves or co-infiltrated with DC*avrRpm1*, or the petiole of the challenged leaf was treated with the inhibitor soaked in cotton wool and secured in place with cling film.

Wounding
Leaf tissue was wounded by crushing either side of the midrib with flat tweezers or by severing the petiole with scissors. Three leaves were wounded per plant, and three biological replicated were imaged.

JAZ10–GUS expression
GUS activity in systemic leaves was assessed at 4, 8 and 24 hpi via GUS staining (1 mM X-Gluc, 100 mM $NaPO_4$ buffer pH 7.0, 10 mM EDTA and 0.1% v/v Triton X-100) using four plants per treatment and challenging four leaves per plant. Samples were incubated at 37 °C. The leaves were de-stained by repeated washes with 70% ethanol, and representative leaf images are shown.

Phenotyping
Infected leaves were removed and imaged at 5.5, 14 and 18 hpi to assess leaf collapse.

Reverse transcription PCR
Total RNA was extracted from mature green leaves of *aos*, *jiss1* and Col-0 (two leaves per plant) using Trizol (Invitrogen, Thermo Fisher Scientific) and treated with DNase I (Merck), according to the manufacturers' instructions. cDNA was synthesized using ReadyScript cDNA Synthesis Mix (Sigma-Aldrich) with both oligo d(T) and random primers and diluted 1:10 for PCR. PCR was performed using BioMix Red 2xPCR mix (Meridian Bioscience) with primers specific to *JISS1* (At5g56980; (LP) CAAGCATGTACGAAGCAAAT; (RP) CTCCTTGTACCTCAGAATCG; amplicon, 301 bp) or *Actin2* (At3g18780; (LP) GCCATCCAAGCTGTTCTCTC; (RP) CAGTAAGGTCACGTCCAGCA; amplicon, 156 bp).

Confocal imaging
Freshly excised leaf samples were mounted in water and imaged on a Zeiss LSM 880 confocal microscope with a ×63 oil-immersion objective (ER images) or a ×10 air objective (whole-leaf images). GFP was excited at 488 nm, and emission was detected in the 498–559 nm range; RFP and chlorophyll A were excited at 561 nm and detected in the 605–649 nm range. For cell wall imaging, petiole sections were stained with an aqueous solution of propidium iodide (25 µM), with excitation at 561 nm and emission detection at 614–659 nm. All image analysis was performed in Fiji (ImageJ2 v.2.9.0/1.53t)[74]. Median pixel (signal) intensity for individual leaves was measured across the defined region of interest with corresponding background subtraction using Fiji.

Electrophysiology experiments
Surface electrical potentials of challenged and systemic leaves were measured following infection using four electrodes (Fig. 5a) adopting a similar approach to ref. 40. The working electrode (W1, red) was always placed on the lamina immediately above the petiole of the challenged leaf. Electrodes W2 (green) and W3 (blue) were placed similarly on adjacent systemic leaves, and W4 (black) on the distal systemic leaf. The reference electrode was placed in the soil. Surface potential changes were measured from the reference electrode to the working electrode. Plants were covered with a propagator lid, electrical recordings were captured using a data logger (PicoLog 1000) and signal amplitude and duration were plotted for each leaf over ~24 h. Control recordings over an extended time predominantly showed a constant surface potential.

Reporting summary
Further information on research design is available in the Nature Portfolio Reporting Summary linked to this article.

Data availability
The dataset for Extended Data Fig. 1 has been deposited at http://affymetrix.arabidopsis.info/narrays under identifier NASCARRAYS-403. The *A. thaliana* reporter lines and all raw data are available from the corresponding author. Source data are provided with this paper. All other data are available in the main text or supplementary materials.

References
1. Cui, J. et al. *Pseudomonas syringae* manipulates systemic plant defenses against pathogens and herbivores. *Proc. Natl Acad. Sci. USA* **102**, 1791–1796 (2005).
2. Shine, M. B., Xiao, X., Kachroo, P. & Kachroo, A. Signaling mechanisms underlying systemic acquired resistance to microbial pathogens. *Plant Sci.* **279**, 81–86 (2019).
3. Riedlmeier, M. et al. Monoterpenes support systemic acquired resistance within and between plants. *Plant Cell* **29**, 1440–1459 (2017).
4. Wang, C. et al. Extracellular pyridine nucleotides trigger plant systemic immunity through a lectin receptor kinase/BAK1 complex. *Nat. Commun.* **10**, 4810 (2019).
5. Shine, M. et al. Phased small RNA–mediated systemic signaling in plants. *Sci. Adv.* **8**, eabm8791 (2022).
6. Liu, H. et al. Piperideine-6-carboxylic acid regulates vitamin B6 homeostasis and modulates systemic immunity in plants. *Nat. Plants* **11**, 263–278 (2025).
7. Wendehenne, D., Gao, Q. M., Kachroo, A. & Kachroo, P. Free radical-mediated systemic immunity in plants. *Curr. Opin. Plant Biol.* **20**, 127–134 (2014).
8. Yu, K. et al. A feedback regulatory loop between G3P and lipid transfer proteins DIR1 and AZI1 mediates azelaic-acid-induced systemic immunity. *Cell Rep.* **3**, 1266–1278 (2013).
9. Gao, Q. M. et al. Mono- and digalactosyldiacylglycerol lipids function nonredundantly to regulate systemic acquired resistance in plants. *Cell Rep.* **9**, 1681–1691 (2014).
10. Kachroo, A. & Kachroo, P. Mobile signals in systemic acquired resistance. *Curr. Opin. Plant Biol.* **58**, 41–47 (2020).
11. Wenig, M. et al. Systemic acquired resistance networks amplify airborne defense cues. *Nat. Commun.* **10**, 3813 (2019).

12. Lim, G.-H. et al. The plant cuticle regulates apoplastic transport of salicylic acid during systemic acquired resistance. *Sci. Adv.* **6**, eaaz0478 (2020).
13. Lim, G.-H. et al. Plasmodesmata localizing proteins regulate transport and signaling during systemic acquired immunity in plants. *Cell Host Microbe* **19**, 541–549 (2016).
14. Shah, J., Chaturvedi, R., Chowdhury, Z., Venables, B. & Petros, R. A. Signaling by small metabolites in systemic acquired resistance. *Plant J.* **79**, 645–658 (2014).
15. Zeier, J. Metabolic regulation of systemic acquired resistance. *Curr. Opin. Plant Biol.* **62**, 102050 (2021).
16. Vlot, A. C. et al. Systemic propagation of immunity in plants. *N. Phytol.* **229**, 1234–1250 (2021).
17. Grant, M. R. et al. Structure of the *Arabidopsis RPM1* gene enabling dual specificity disease resistance. *Science* **269**, 843–846 (1995).
18. Grant, M. et al. The *RPM1* plant disease resistance gene facilitates a rapid and sustained increase in cytosolic calcium that is necessary for the oxidative burst and hypersensitive cell death. *Plant J.* **23**, 441–450 (2000).
19. Jacob, P. et al. Plant 'helper' immune receptors are Ca^{2+}-permeable nonselective cation channels. *Science* **373**, 420–425 (2021).
20. Bennett, M., Mehta, M. & Grant, M. Biophoton imaging: a nondestructive method for assaying R gene responses. *Mol. Plant Microbe Interact.* **18**, 95–102 (2005).
21. Birtic, S. et al. Using spontaneous photon emission to image lipid oxidation patterns in plant tissues. *Plant J.* **67**, 1103–1115 (2011).
22. Truman, W., Bennett, M. H., Kubigsteltig, I., Turnbull, C. & Grant, M. *Arabidopsis* systemic immunity uses conserved defense signaling pathways and is mediated by jasmonates. *Proc. Natl Acad. Sci. USA* **104**, 1075–1080 (2007).
23. Kiep, V. et al. Systemic cytosolic Ca(2+) elevation is activated upon wounding and herbivory in *Arabidopsis*. *N. Phytol.* **207**, 996–1004 (2015).
24. Kiefer, I. W. & Slusarenko, A. J. The pattern of systemic acquired resistance induction within the *Arabidopsis* rosette in relation to the pattern of translocation. *Plant Physiol.* **132**, 840–847 (2003).
25. Bent, A. F. et al. RPS2 of *Arabidopsis thaliana*: a leucine-rich repeat class of plant disease resistance genes. *Science* **265**, 1856–1860 (1994).
26. Gassmann, W., Hinsch, M. E. & Staskawicz, B. J. The *Arabidopsis* RPS4 bacterial-resistance gene is a member of the TIR–NBS–LRR family of disease-resistance genes. *Plant J.* **20**, 265–277 (1999).
27. Littlejohn, G. R., Breen, S., Smirnoff, N. & Grant, M. Chloroplast immunity illuminated. *N. Phytol.* https://doi.org/10.1111/nph.17076 (2020).
28. Fu, Z. Q. et al. NPR3 and NPR4 are receptors for the immune signal salicylic acid in plants. *Nature* **486**, 228–232 (2012).
29. Rate, D. N. & Greenberg, J. T. The *Arabidopsis aberrant growth and death2* mutant shows resistance to *Pseudomonas syringae* and reveals a role for NPR1 in suppressing hypersensitive cell death. *Plant J.* **27**, 203–211 (2001).
30. Cao, H., Bowling, S. A., Gordon, A. S. & Dong, X. Characterization of an *Arabidopsis* mutant that is nonresponsive to inducers of systemic acquired resistance. *Plant Cell* **6**, 1583–1592 (1994).
31. Liu, L. et al. Salicylic acid receptors activate jasmonic acid signalling through a non-canonical pathway to promote effector-triggered immunity. *Nat. Commun.* **7**, 13099 (2016).
32. Zheng, X. Y. et al. Coronatine promotes *Pseudomonas syringae* virulence in plants by activating a signaling cascade that inhibits salicylic acid accumulation. *Cell Host Microbe* **11**, 587–596 (2012).
33. Wildermuth, M. C., Dewdney, J., Wu, G. & Ausubel, F. M. Isochorismate synthase is required to synthesize salicylic acid for plant defence. *Nature* **414**, 562–565 (2001).
34. Hartmann, M. et al. Flavin monooxygenase-generated *N*-hydroxypipecolic acid is a critical element of plant systemic immunity. *Cell* **173**, 456–469 e416 (2018).
35. Thines, B. et al. JAZ repressor proteins are targets of the SCFCOI1 complex during jasmonate signalling. *Nature* **448**, 661–665 (2007).
36. Katsir, L., Schilmiller, A. L., Staswick, P. E., He, S. Y. & Howe, G. A. COI1 is a critical component of a receptor for jasmonate and the bacterial virulence factor coronatine. *Proc. Natl Acad. Sci. USA* **105**, 7100–7105 (2008).
37. Torres Zabala, M. et al. Novel JAZ co-operativity and unexpected JA dynamics underpin *Arabidopsis* defence responses to *Pseudomonas syringae* infection. *N. Phytol.* **209**, 1120–1134 (2015).
38. Brooks, D. M. et al. Identification and characterization of a well-defined series of coronatine biosynthetic mutants of *Pseudomonas syringae* pv. *tomato* DC3000. *Mol. Plant Microbe Interact.* **17**, 162–174 (2004).
39. Zhang, L., Zhang, F., Melotto, M., Yao, J. & He, S. Y. Jasmonate signaling and manipulation by pathogens and insects. *J. Exp. Bot.* **68**, 1371–1385 (2017).
40. Mousavi, S. A., Chauvin, A., Pascaud, F., Kellenberger, S. & Farmer, E. E. GLUTAMATE RECEPTOR-LIKE genes mediate leaf-to-leaf wound signalling. *Nature* **500**, 422–426 (2013).
41. Ellis, C. & Turner, J. A conditionally fertile *coi1* allele indicates cross-talk between plant hormone signalling pathways in *Arabidopsis thaliana* seeds and young seedlings. *Planta* **215**, 549–556 (2002).
42. Park, J. H. et al. A knock-out mutation in allene oxide synthase results in male sterility and defective wound signal transduction in *Arabidopsis* due to a block in jasmonic acid biosynthesis. *Plant J.* **31**, 1–12 (2002).
43. Li, M., Yu, G., Cao, C. & Liu, P. Metabolism, signaling, and transport of jasmonates. *Plant Commun.* **2**, 100231 (2021).
44. Wasternack, C. & Song, S. Jasmonates: biosynthesis, metabolism, and signaling by proteins activating and repressing transcription. *J. Exp. Bot.* **68**, 1303–1321 (2017).
45. Cucurou, C., Battioni, J. P., Thang, D. C., Nam, N. H. & Mansuy, D. Mechanisms of inactivation of lipoxygenases by phenidone and BW755C. *Biochemistry* **30**, 8964–8970 (1991).
46. Farmer, E. E., Caldelari, D., Pearce, G., Walker-Simmons, M. K. & Ryan, C. A. Diethyldithiocarbamic acid inhibits the octadecanoid signaling pathway for the wound induction of proteinase inhibitors in tomato leaves. *Plant Physiol.* **106**, 337–342 (1994).
47. Meesters, C. et al. A chemical inhibitor of jasmonate signaling targets JAR1 in *Arabidopsis thaliana*. *Nat. Chem. Biol.* **10**, 830–836 (2014).
48. Nguyen, C. T., Kurenda, A., Stolz, S., Chetelat, A. & Farmer, E. E. Identification of cell populations necessary for leaf-to-leaf electrical signaling in a wounded plant. *Proc. Natl Acad. Sci. USA* **115**, 10178–10183 (2018).
49. Choi, W. G., Hilleary, R., Swanson, S. J., Kim, S. H. & Gilroy, S. Rapid, long-distance electrical and calcium signaling in plants. *Annu. Rev. Plant Biol.* **67**, 287–307 (2016).
50. Toyota, M. et al. Glutamate triggers long-distance, calcium-based plant defense signaling. *Science* **361**, 1112–1115 (2018).
51. Yan, C. et al. Ca(2+)/calmodulin-mediated desensitization of glutamate receptors shapes plant systemic wound signalling and anti-herbivore defence. *Nat. Plants* **10**, 145–160 (2024).
52. Wang, J., Song, W. & Chai, J. Structure, biochemical function, and signaling mechanism of plant NLRs. *Mol. Plant* **16**, 75–95 (2023).
53. de Torres-Zabala, M. et al. Chloroplasts play a central role in plant defence and are targeted by pathogen effectors. *Nat. Plants* **1**, 15074 (2015).
54. Mur, L. A., Kenton, P., Atzorn, R., Miersch, O. & Wasternack, C. The outcomes of concentration-specific interactions between salicylate and jasmonate signaling include synergy, antagonism, and oxidative stress leading to cell death. *Plant Physiol.* **140**, 249–262 (2006).

55. Jacob, P., Hige, J. & Dangl, J. L. Is localized acquired resistance the mechanism for effector-triggered disease resistance in plants? *Nat. Plants* https://doi.org/10.1038/s41477-023-01466-1 (2023).
56. Betsuyaku, S. et al. Salicylic acid and jasmonic acid pathways are activated in spatially different domains around the infection site during effector-triggered immunity in *Arabidopsis thaliana*. *Plant Cell Physiol.* **59**, 8–16 (2018).
57. Andersson, M. X. et al. Oxylipin profiling of the hypersensitive response in *Arabidopsis thaliana*: formation of a novel oxo-phytodienoic acid-containing galactolipid, arabidopside E. *J. Biol. Chem.* **281**, 31528–31537 (2006).
58. Zoeller, M. et al. Lipid profiling of the *Arabidopsis* hypersensitive response reveals specific lipid peroxidation and fragmentation processes: biogenesis of pimelic and azelaic acid. *Plant Physiol.* **160**, 365–378 (2012).
59. Li, Q., Wang, C. & Mou, Z. Perception of damaged self in plants. *Plant Physiol.* **182**, 1545–1565 (2020).
60. Vega-Munoz, I. et al. Breaking bad news: dynamic molecular mechanisms of wound response in plants. *Front. Plant Sci.* **11**, 610445 (2020).
61. Yuan, M., Ngou, B. P. M., Ding, P. & Xin, X. F. PTI–ETI crosstalk: an integrative view of plant immunity. *Curr. Opin. Plant Biol.* **62**, 102030 (2021).
62. Bjornson, M., Pimprikar, P., Nurnberger, T. & Zipfel, C. The transcriptional landscape of *Arabidopsis thaliana* pattern-triggered immunity. *Nat. Plants* **7**, 579–586 (2021).
63. Manzoor, H. et al. Involvement of the glutamate receptor AtGLR3.3 in plant defense signaling and resistance to *Hyaloperonospora arabidopsidis*. *Plant J.* **76**, 466–480 (2013).
64. Perkins, L. E. et al. Generalist insects behave in a jasmonate-dependent manner on their host plants, leaving induced areas quickly and staying longer on distant parts. *Proc. R. Soc. B* **280**, 20122646 (2013).
65. Morin, H. et al. Wound-response jasmonate dynamics in the primary vasculature. *N. Phytol.* **240**, 1484–1496 (2023).
66. Gilroy, S. et al. ROS, calcium, and electric signals: key mediators of rapid systemic signaling in plants. *Plant Physiol.* **171**, 1606–1615 (2016).
67. de Torres, M. et al. *Pseudomonas syringae* effector AvrPtoB suppresses basal defence in *Arabidopsis*. *Plant J.* **47**, 368–382 (2006).
68. Procko, C. et al. Leaf cell-specific and single-cell transcriptional profiling reveals a role for the palisade layer in UV light protection. *Plant Cell* **34**, 3261–3279 (2022).
69. Clough, S. J. & Bent, A. F. Floral dip: a simplified method for *Agrobacterium*-mediated transformation of *Arabidopsis thaliana*. *Plant J.* **16**, 735–743 (1998).
70. O'Malley, R. C., Alonso, J. M., Kim, C. J., Leisse, T. J. & Ecker, J. R. An adapter ligation-mediated PCR method for high-throughput mapping of T-DNA inserts in the *Arabidopsis* genome. *Nat. Protoc.* **2**, 2910–2917 (2007).
71. Engler, C. et al. A Golden Gate modular cloning toolbox for plants. *ACS Synth. Biol.* **3**, 839–843 (2014).
72. King, E. O., Ward, M. K. & Raney, D. E. Two simple media for the demonstration of pyocyanin and fluorescin. *J. Lab. Clin. Med.* **44**, 301–307 (1954).
73. Rufian, J. S., Rueda-Blanco, J., Beuzon, C. R. & Ruiz-Albert, J. Protocol: an improved method to quantify activation of systemic acquired resistance (SAR). *Plant Methods* **15**, 16 (2019).
74. Schindelin, J. et al. Fiji: an open-source platform for biological-image analysis. *Nat. Methods* **9**, 676–682 (2012).

Acknowledgements

We thank R. Winsbury (Exeter) for technical help and P. Winlove and S. Green (Exeter) for electrophysiology advice. C. Gall helped with figure preparations. T.G. was supported by an Indian Government PhD studentship. M.G. acknowledges support from BBSRC/UKRI grant nos BB/P002560/1 and BB/X013049/1, the Leverhulme Trust (grant no. RPG-2013-275), the National Science Foundation (grant no. MCB-2435880) and a BBSRC IAA award (no. BB/S506783/1) to the Warwick Bio-electrical Engineering Hub. E.B., M.G. and L.F. acknowledge support from BBSRC/UKRI grant no. BB/W007126/1.

Author contributions

M.G., M.d.T.-Z., T.G., S.B., E.B. and E.S. conceptualized and designed the experiments. T.G., S.B., E.B., R.H., N.K., F.B. and E.S. performed the experiments and analysed the data. T.G., M.d.T.-Z., F.B., R.H. and S.K. generated the material and resources. D.H. designed the equipment and L.F., P.K. and D.H. provided experimental insights. M.G., S.B., E.B., E.S. and P.K. wrote the manuscript. M.G. and P.K. provided financial support.

Competing interests

The authors declare no competing interests.

Additional information

Extended data is available for this paper at https://doi.org/10.1038/s41477-025-02178-4.

Supplementary information The online version contains supplementary material available at https://doi.org/10.1038/s41477-025-02178-4.

Correspondence and requests for materials should be addressed to Murray Grant.

Peer review information *Nature Plants* thanks the anonymous reviewers for their contribution to the peer review of this work.

Reprints and permissions information is available at www.nature.com/reprints.

Publisher's note Springer Nature remains neutral with regard to jurisdictional claims in published maps and institutional affiliations.

[1]School of Life Sciences, University of Warwick, Coventry, UK. [2]Biopharm Discovery, GlaxoSmithKline, Stevenage, UK. [3]Biosciences, College of Life and Environmental Sciences, University of Exeter, Exeter, UK. [4]College of Engineering, Maths & Physical Sciences, University of Exeter, Exeter, UK. [5]Department of Plant Pathology, University of Kentucky, Lexington, KY, USA. [6]Present address: Marine Biology Association, Plymouth, UK. [7]Present address: Department of Cell and Molecular Sciences, James Hutton Institute, Invergowrie, UK. [8]These authors contributed equally: Trupti Gaikwad, Susan Breen, Emily Breeze, Erin Stroud. ✉e-mail: m.grant@warwick.ac.uk

https://doi.org/10.1038/s41477-025-02178-4

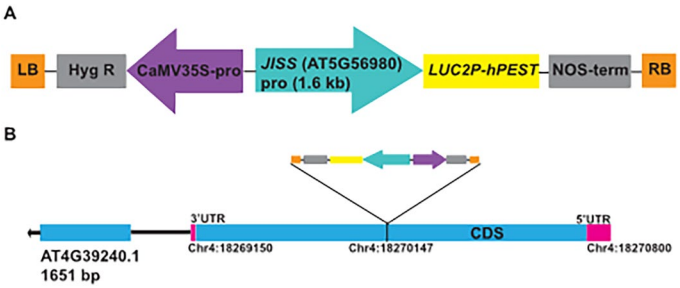

Extended Data Fig. 1 | Schematic of the *JISS1:LUC* construct and its T-DNA integration location in the *Arabidopsis* genome. (**A**). The *Photinus pyralis LUC2P* reporter gene (from Promega pGL4-11) was PCR amplified and cloned into pCAMBIA1302 digested with Kpn1 and Pml1 to generate pC1LUCP with a *NOS* terminator. A 1651 bp *JISS1* fragment containing the promoter and encoding the first 84aa of JISS1 was PCR amplified as described[64] generating a hygromycin selectable *JISS1:LUC* construct. (**B**) Eight independent homozygous lines *A. thaliana* Col-5 *JISS1:LUC* expressing transgenic lines were generated and tested for luciferase expression in systemic leaves following an immunising challenge with DC*avrRpm1*. A homozygous line showing strong *JISS1:LUC* expression was chosen and the genomic location of the *JISS1:LUC* T-DNA construct was determined at position 18270147 in the coding region of AT4G39240.1 sequence analysis as per[70].

https://doi.org/10.1038/s41477-025-02178-4

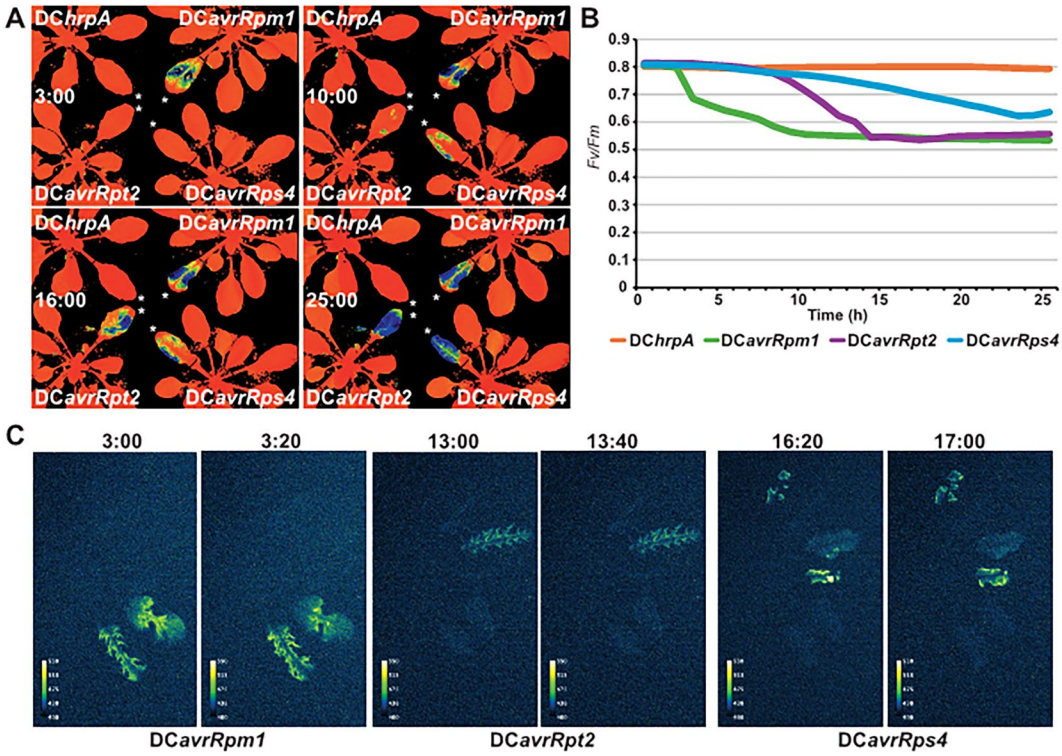

Extended Data Fig. 2 | DC*avrRpt2* F_v/F_m dynamics and biophoton generation is earlier than DC*avrRps4* although its systemic *JISS1:LUC* expression is considerably later. (**A, B**) Visualisation (**A**) and quantitation (**B**) of F_v/F_m suppression within a plant over infection time showing, like with biophoton generation (**C**), ETI elicited by DC*avrRpt2* affects chloroplast physiology (PSII) faster than DC*avrRps4* challenge. In (**A**) orange represents a healthy PSII signature whereas blue signifies strongly disrupted PSII due to ETI induced ROS. (**C**) The sequence of biophoton generation, matches F_v/F_m suppression, during ETI elicited by DC*avrRpm1*, DC*avrRpt2* or DC*avrRps4* challenge (times indicated). Stills taken from Supplementary Video 2.

https://doi.org/10.1038/s41477-025-02178-4

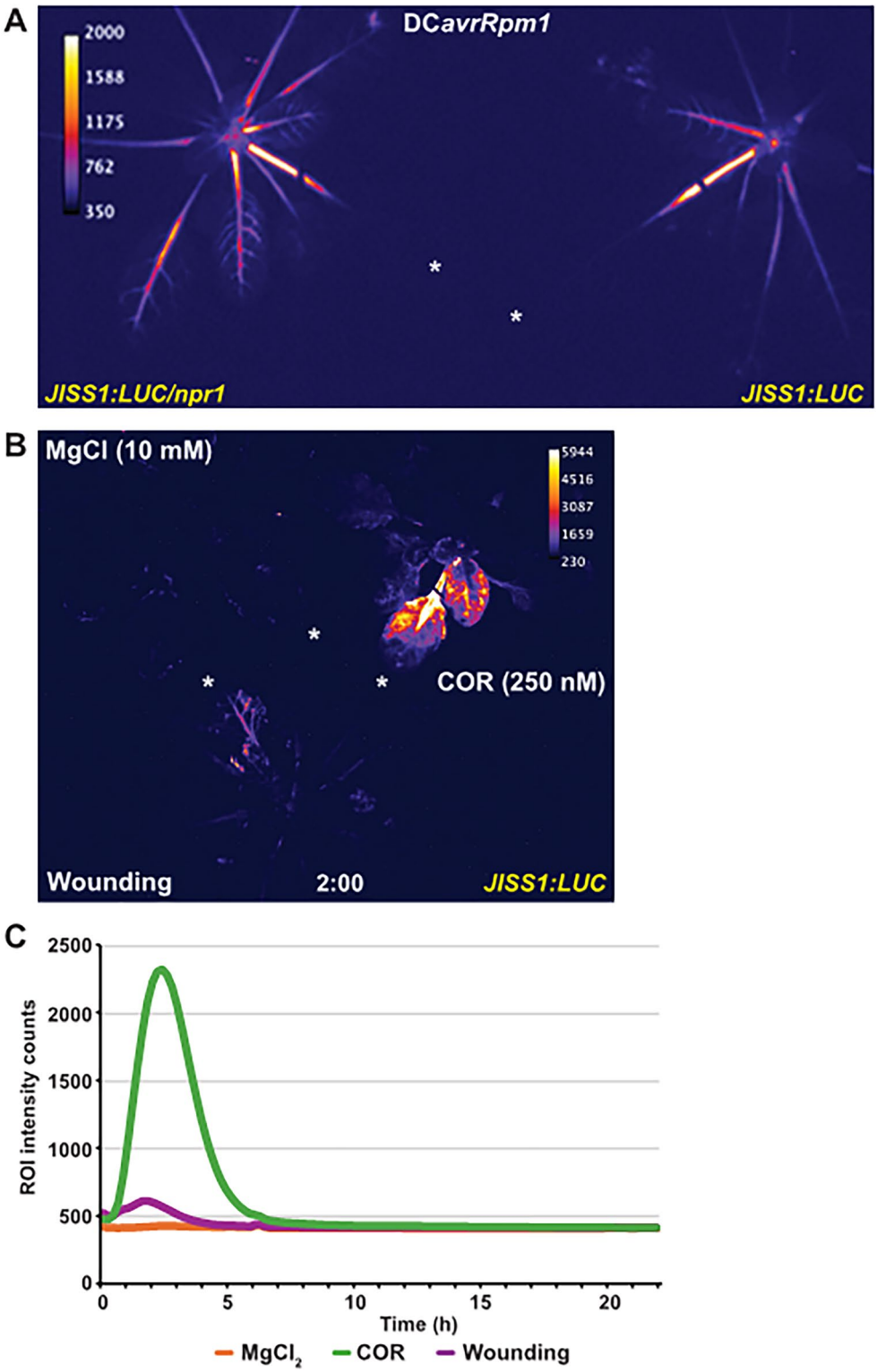

Extended Data Fig. 3 | *JISS1* signal propagation is not impaired in *npr1*, but responds to wounding and the JA elicitor coronatine. A white asterisk denotes treated leaves and images are false coloured by signal intensity, indicated by the calibration bar. (**A**) A *JISS1:LUC/npr1* line exhibited comparable systemic luciferase activity to the wild-type Col-0 *JISS1:LUC* line following DC*avrRpm1* challenge (4:20 hpi). (**B**, **C**) Strong and transient luciferase activity was observed in response to 250 nM coronatine (COR), a milder response was triggered by wounding and no response was detected following mock treatment (10 mM $MgCl_2$) 2 hpi.

https://doi.org/10.1038/s41477-025-02178-4

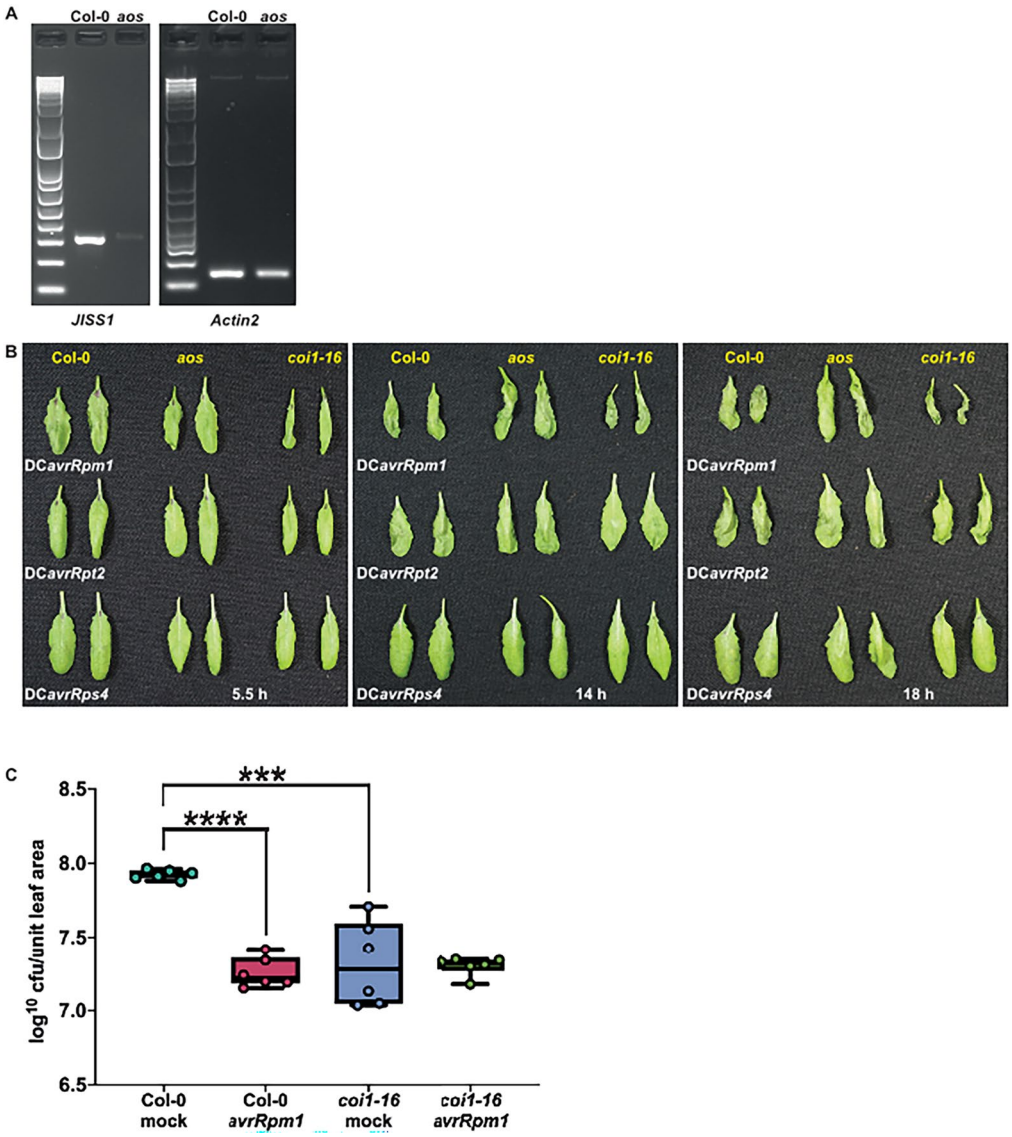

Extended Data Fig. 4 | HR development is not affected in mutants with impaired JA biosynthesis (*aos*) or perception (*coi1-16*) but *coi1-16* has reduced disease susceptibility. (**A**) RT-PCR verification loss of *JISS1* expression in the *aos* T-DNA insertion line. *Actin2* expression was used as a loading control (**B**) Phenotyping of Col-0 and *aos* and *coi1-16* mutants showing that loss of JA biosynthesis and signalling does not affect HR development. (**C**) SAR growth curve of *Psm4* following DC*avrRpm1* or mock pre-treatment on Col-0 (**** p = <0.0001, t = 15.36, df=10 [unpaired t test]) and the *coi1-16* mutant (p = 0.9421, t = 0.07450, df=10). *coi1-16* is more resistant to *Psm4* than wild-type Col-0 (*** p = 0.0004, t = 5.154, df=10) (n = 6 biological replicates). Col-0 mock: min=7.88, max=7.96, median=7.92, Q1 = 7.91, Q3 = 7.94; Col-0 DC*avrRpm1*: min=7.15, max=7.42, median=7.22, Q1 = 7.19, Q3 = 7.31; *coi1-16* mock: min=7.03, max=7.71, median=7.28, Q1 = 7.07, Q3 = 7.53; *coi1-16* DC*avrRpm1*: min=7.19, max=7.36, median=7.33, Q1 = 7.31, Q3 = 7.35.

https://doi.org/10.1038/s41477-025-02178-4

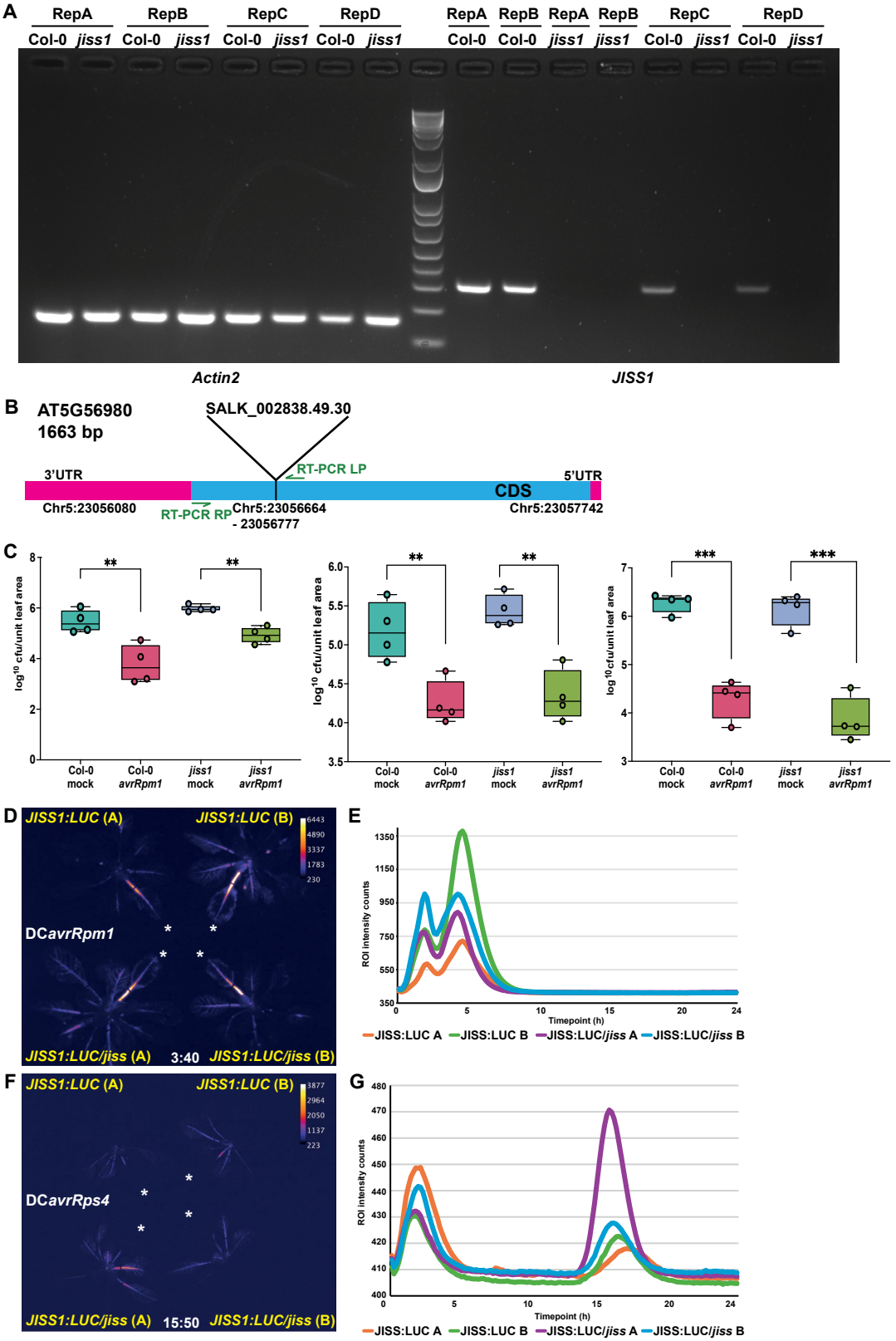

Extended Data Fig. 5 | See next page for caption.

https://doi.org/10.1038/s41477-025-02178-4

Extended Data Fig. 5 | *jiss1* mutants do not impact SAR and the *JISS1* protein is not required for systemic signalling. (**A**) RT-PCR verification loss of *JISS1* expression in the *jiss1* T-DNA insertion line. *Actin2* expression was used as a loading control. **(B)** T-DNA insertion in the coding sequence of the *JISS1* gene (AT5G56980) is located at position Chr5: 23056664–23056777. Relative positions of forward and reverse gene specific RT-PCR primers are indicated, and sequences are given in Methods. **(C)** SAR growth curve of DC following DC*avrRpm1* or mock pre-treatment on wild-type (Col-0) and the *jiss1* mutant (n = 4 biological replicates). **Replicate 1:** Col-0 ** p = 0.0094, t = 3.759, df=6 [unpaired two-tailed t test], *jiss1* ** p = 0.0010, t = 5.943, df=6 [unpaired two-tailed t test]. Col-0 mock: min=5.06, max=6.05, median=5.37, Q1 = 5.12, Q3 = 5.71; Col-0 DC*avrRpm1*: min=3.09, max=4.73, median=3.64, Q1 = 3.18, Q3 = 4.24; *jiss 1* mock: min=5.86, max=6.16, median=5.94, Q1 = 5.92, Q3 = 6.00; *jiss1* DC*avrRpm1*: min=4.56, max=5.31, median=4.92, Q1 = 4.72, Q3 = 5.12. **Replicate 2:** Col-0 ** p = 0.0076, t = 3.947, df=6 [unpaired two-tailed t test], *jiss1* ** p = 0.0015, t = 5.498, df=6 [unpaired two-tailed t test]) Col-0 mock: min=4.78, max=5.65, median=5.15, Q1 = 4.94, Q3 = 5.39; Col-0 DC*avrRpm1*: min=4.02, max=4.66, median=4.16, Q1 = 4.11, Q3 = 4.31; *jiss 1* mock: min=5.26, max=5.72, median=5.38, Q1 = 5.27, Q3 = 5.53; *jiss1* DC*avrRpm1*: min=4.02, max=4.81, median=4.28, Q1 = 4.17, Q3 = 4.45. **Replicate 3:** Col-0 *** p = 0.0001, t = 8.699, df=6 [unpaired two-tailed t test], *jiss1* *** p = 0.0002, t = 7.951, df=6 [unpaired two-tailed t test]. Col-0 mock: min=5.97, max=6.42, median=6.35, Q1 = 6.25, Q3 = 6.37; Col-0 DC*avrRpm1*: min=3.70, max=4.63, median=4.41, Q1 = 4.21, Q3 = 4.49; *jiss 1* mock: min=5.64, max=6.40, median=6.28, Q1 = 6.09, Q3 = 6.34; *jiss1* DC*avrRpm1*: min=3.45, max=4.52, median=3.72, Q1 = 3.65, Q3 = 3.93. **(D-G)** The *JISS1:LUC* reporter in the *jiss1* mutant responds as wild type following challenge with either DC*avrRpm1* (**D**-**E**) or DC*avrRps4* (**F**-**G**). A white asterisk denotes infiltrated leaves and images are false coloured by signal intensity, as indicated by calibration bar. Luciferase activity shows similar dynamics and signal intensity in response to DC*avrRpm1* (**D**-**E**) and DC*avrRps4* (**F**-**G**) in *JISS1:LUC* and *JISS1:LUC/jiss1* lines.

https://doi.org/10.1038/s41477-025-02178-4

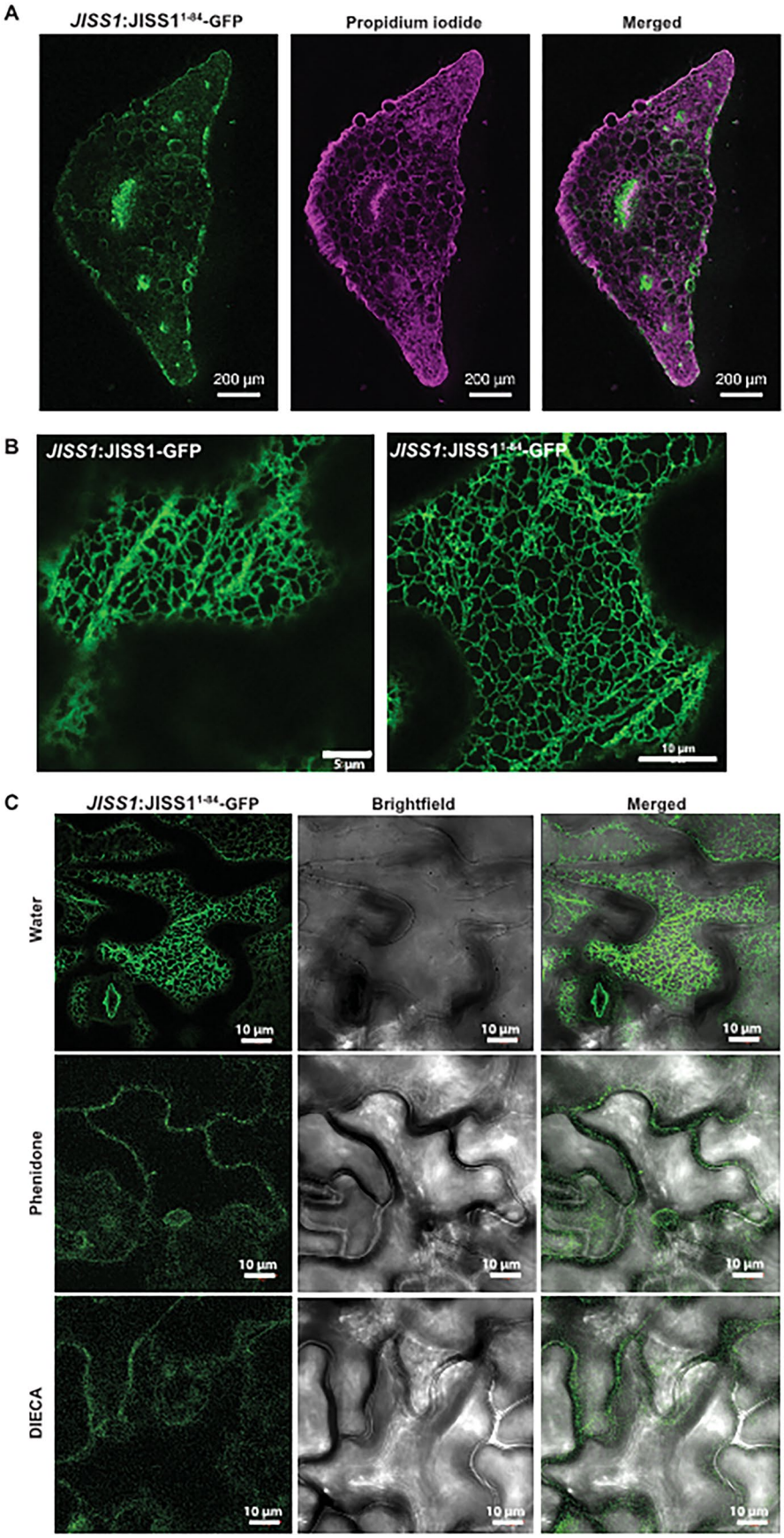

Extended Data Fig. 6 | See next page for caption.

https://doi.org/10.1038/s41477-025-02178-4

Extended Data Fig. 6 | JA dependent localisation of *JISS1*:JISS1$^{1-84}$-*GFP* and *JISS1*:JISS1-*GFP* in systemic tissue. (**A**) Petiole section from systemic leaf showing propidium iodide staining (magenta) and *JISS1*:JISS1$^{1-84}$-*GFP* expression (green) with merged image. Scale bar, 200 µm (**B**) Representative confocal images of *JISS1*:JISS1-GFP and *JISS1*:JISS1$^{1-84}$-GFP plants following DC*avrRpm1* challenge, showing identical subcellular localisation of GFP in ER network of epidermal cells. Scale bars, 5 µm and 10 µm, respectively. **(C)** Representative confocal images of Arabidopsis epidermal leaf cells of *JISS1*:JISS1$^{1-84}$-GFP systemic leaves pre-treated with JA inhibitors, phenidone (2 mM) and DIECA (2.5 mM) prior to DC*avrRpm1* challenge or mock treated. Mock treatment of systemic leaves shows JISS1$^{1-84}$-GFP labelling of the entire ER network 4 hpi whereas Systemic leaves infiltrated with phenidone or DIECA exhibit strongly reduced GFP signal in the ER 4 hpi compared to signal across the entire ER network after mock treatment. Scale bar, 10 µm. Images are representative of at least 3 biological replicates.

https://doi.org/10.1038/s41477-025-02178-4

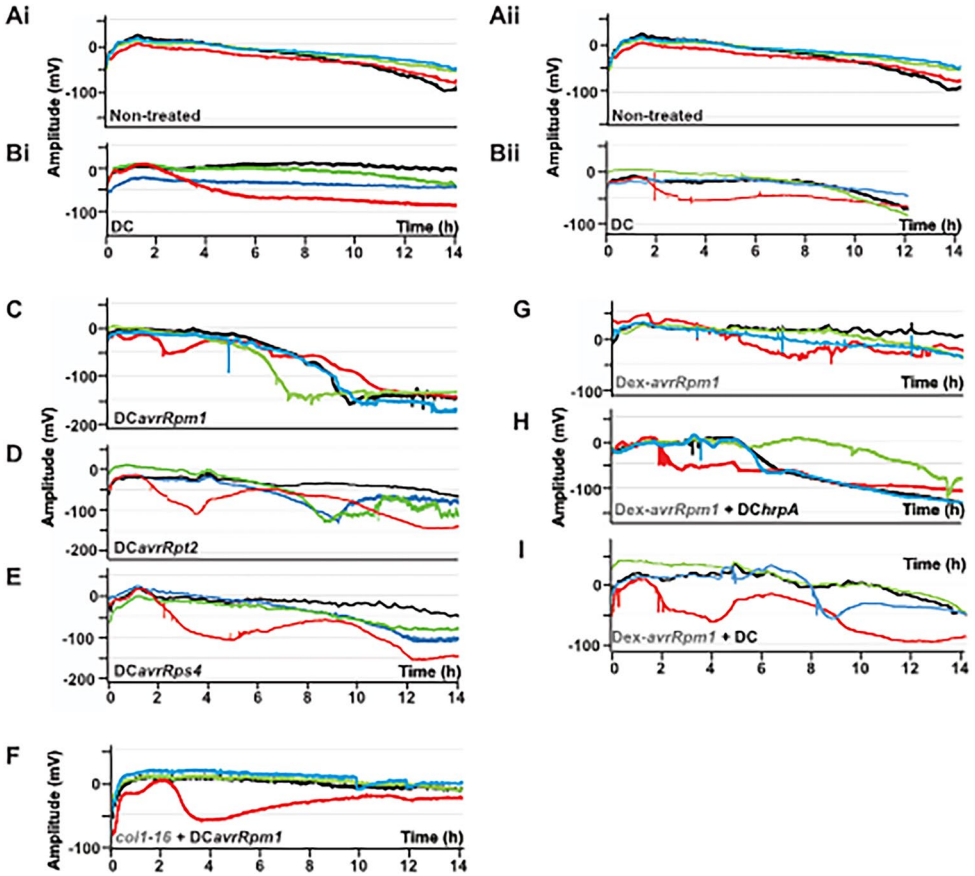

Extended Data Fig. 7 | ETI activation of systemic electric signalling is consistent. Replicated data displayed consistent with Fig. 5. (**A**) Col-0 plants do not show development of SISPs in non-treated plants. (**B**) Col-0 plants do not show development of SISPs following DC challenge. (**C-E**) Challenge with DC*avrRpm1*, DC*avrRpt2*, and DC*avrRps4* exhibits depolarisation of the infected leaf from 2 hpi, followed by induction of SISPs from 6-10 hpi. (**F**) Infiltration of DC*avrRpm1* in the *coi1-16* mutant causes transient depolarization (3-4 hpi) in the challenged but not distal nor adjacent leaves. (**G**) Dex-avrRpm1 plants do not show SISPs in non-treated plants. (**H-I**) Infiltration of DC*hrpA* or DC 1 h after Dex induction of *avrRpm1* induces depolarisation and repolarisation of the infiltrated leaf and initiation of SISPs in some systemic responding leaves, albeit weaker than DC*avrRpm1*.

https://doi.org/10.1038/s41477-025-02178-4

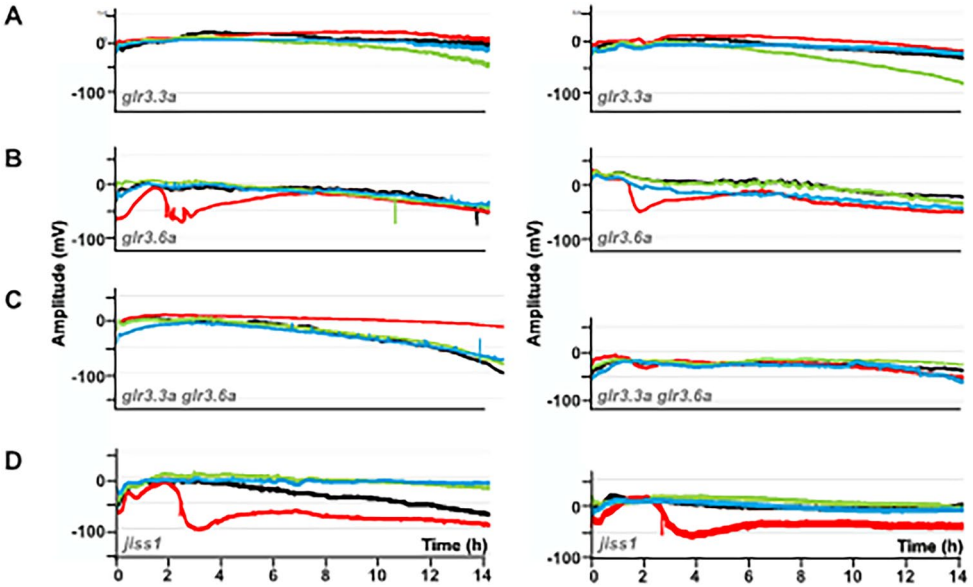

Extended Data Fig. 8 | ETI activation of systemic electric signalling is consistent. Replicated data (n = 2) displayed consistent SISP signatures to Fig. 6. (**A**) Challenge of *glr3.3a* with DC*avrRpm1* does not show SISPs. (**B**) Challenge of *glr3.6a* with DC*avrRpm1* shows limited depolarization in the infiltrated but not distal leaves. (**C**) Challenge of *glr3.3a glr3.6a* with DC*avrRpm1* does not show SISPs. (**D**) Challenge of *jiss1* with DC*avrRpm1* shows limited depolarization in the infiltrated but not distal leaves.

nature portfolio

Corresponding author(s): Murray Grant

Last updated by author(s): 7th November 2025

Reporting Summary

Nature Portfolio wishes to improve the reproducibility of the work that we publish. This form provides structure for consistency and transparency in reporting. For further information on Nature Portfolio policies, see our Editorial Policies and the Editorial Policy Checklist.

Statistics

For all statistical analyses, confirm that the following items are present in the figure legend, table legend, main text, or Methods section.

n/a	Confirmed	
☐	☒	The exact sample size (*n*) for each experimental group/condition, given as a discrete number and unit of measurement
☒	☐	A statement on whether measurements were taken from distinct samples or whether the same sample was measured repeatedly
☐	☒	The statistical test(s) used AND whether they are one- or two-sided *Only common tests should be described solely by name; describe more complex techniques in the Methods section.*
☒	☐	A description of all covariates tested
☒	☐	A description of any assumptions or corrections, such as tests of normality and adjustment for multiple comparisons
☒	☐	A full description of the statistical parameters including central tendency (e.g. means) or other basic estimates (e.g. regression coefficient) AND variation (e.g. standard deviation) or associated estimates of uncertainty (e.g. confidence intervals)
☐	☒	For null hypothesis testing, the test statistic (e.g. *F*, *t*, *r*) with confidence intervals, effect sizes, degrees of freedom and *P* value noted *Give P values as exact values whenever suitable.*
☒	☐	For Bayesian analysis, information on the choice of priors and Markov chain Monte Carlo settings
☒	☐	For hierarchical and complex designs, identification of the appropriate level for tests and full reporting of outcomes
☒	☐	Estimates of effect sizes (e.g. Cohen's *d*, Pearson's *r*), indicating how they were calculated

Our web collection on statistics for biologists contains articles on many of the points above.

Software and code

Policy information about availability of computer code

Data collection	Chlorophyll fluorescence measurements were carried out using a CF Imager (Technologica Ltd, Colchester, UK) and data extracted and analysed using the FluorImager software V2.305. Luciferase visualisation and biophoton data acquisition was performed using Micro-Manager 1.4 (QImaging)
Data analysis	Image analysis (confocal and biophotons) was performed using Fiji (ImageJ2 version 2.9.0/1.53t)

For manuscripts utilizing custom algorithms or software that are central to the research but not yet described in published literature, software must be made available to editors and reviewers. We strongly encourage code deposition in a community repository (e.g. GitHub). See the Nature Portfolio guidelines for submitting code & software for further information.

Data

Policy information about availability of data

All manuscripts must include a data availability statement. This statement should provide the following information, where applicable:

- Accession codes, unique identifiers, or web links for publicly available datasets
- A description of any restrictions on data availability
- For clinical datasets or third party data, please ensure that the statement adheres to our policy

All data is available in the main text or the supplementary materials. Arabidopsis thaliana reporter lines are available from the corresponding author.

Research involving human participants, their data, or biological material

Policy information about studies with human participants or human data. See also policy information about sex, gender (identity/presentation), and sexual orientation and race, ethnicity and racism.

Reporting on sex and gender	N/A
Reporting on race, ethnicity, or other socially relevant groupings	N/A
Population characteristics	N/A
Recruitment	N/A
Ethics oversight	N/A

Note that full information on the approval of the study protocol must also be provided in the manuscript.

Field-specific reporting

Please select the one below that is the best fit for your research. If you are not sure, read the appropriate sections before making your selection.

☒ Life sciences ☐ Behavioural & social sciences ☐ Ecological, evolutionary & environmental sciences

For a reference copy of the document with all sections, see nature.com/documents/nr-reporting-summary-flat.pdf

Life sciences study design

All studies must disclose on these points even when the disclosure is negative.

Sample size	Chlorophyll fluorescence, biophotons, and luciferase imaging: Sample size per experiment is limited to 4 plants due to the size constraints of the imaging cabinet. Each experiment was performed at least 3 times (and often in excess of 10 times) with comparable results. Confocal microscopy: JISS1:JISS1-GFP lines were imaged on several occasions with multiple epidermal cells viewed each time and images captured from n=8-10 representative cells/experiment. Electrophysiology: Due to the nature of the experimental set up it is only possible to capture measurements from one plant per experiment, hence the data was obtained from n=1. However, each of the presented experiments was repeated multiple times with comparable traces produced, as shown in the Extended Data. SAR growth assays: Each SAR experiment used 6 plants per mutant as determined by practical experimental constraints. Each experiment was repeated at least 3 times, and the SAR experiments on the jiss1 mutant were completed more than 10 times in two independent laboratories using similar protocols (detailed in methodology). JAZ10:GUS expression: For each bacterial treatment (DChrpA, DCavrRpm1 or DC) four leaves on four plants (JAZ10:GUS Col-0 or JAZ10:GUS coi1-16) were challenged. At each timepoint (4h, 6h, 8h) one unchallenged (systemic) leaf was harvested from each plant and assayed for GUS activity. Two representative images from the four assayed leaves are shown in Fig 3A. RT-PCR: RNA was extracted from leaf material from n=3-4 plants (2 leaves per plant) with 3 independent batches of plants grown in total ie n=9-12 (Note: this was part of a larger experiment where some plants were infected with DC3000, hence the high level of replication)
Data exclusions	SAR assays are known to be highly variable (Rufian et al., 2019). Each SAR experiment was performed on n=6 plant/treatment/mutant. We pre-established exclusion criteria such that data would be excluded from 1. any plant exhibiting secondary (opportunistic) fungal infection 2. any plant exhibiting bacterial counts at least 1 log fold base 10 different to the median of the remaining plants with a maximum of 2 plants excluded from each mutant/treatment group (ie minimum of n=4); if n<4 following this exclusion criteria then the whole experiment was discarded and repeated.
Replication	Biophoton experiments are variable in terms of the exact timings when the signal is observed (typically within a 2 hour window) but also in that some infiltrated leaves do not produce a detectable biophoton signal. On occasion it was therefore not possible to observe detectable signals from all three bacterial challenges on the same plant in order to produce a single figure panel (as presented in Extended Data Fig. 2C). However, we consistently saw leaves producing a biophoton signal in the temporal order presented ie DCavrRpm1, then DCavrRpt2 then DCavrRps4. The exact timing of signal generation was also highly consistent between plants in the same experiment.
Randomization	Trays of 24 Arabidopsis plants/line are grown under controlled conditions for 5-6 weeks prior to experimentation. Plants within a tray are thus highly comparable in terms of growth and development. Multiple plants from the same tray are selected for an experiment and randomly

assigned to a treatment group. Where multiple lines are used in an experiment all plants were sown on the same day and grown under the same conditions thus ensuring inter-line consistency in growth and development.

Blinding: Blinding was not performed due to researcher personnel constraints and the need to ensure adequate sample labelling and tracking.

Reporting for specific materials, systems and methods

We require information from authors about some types of materials, experimental systems and methods used in many studies. Here, indicate whether each material, system or method listed is relevant to your study. If you are not sure if a list item applies to your research, read the appropriate section before selecting a response.

Materials & experimental systems

n/a	Involved in the study
☒	☐ Antibodies
☒	☐ Eukaryotic cell lines
☒	☐ Palaeontology and archaeology
☐	☒ Animals and other organisms
☒	☐ Clinical data
☒	☐ Dual use research of concern
☐	☒ Plants

Methods

n/a	Involved in the study
☒	☐ ChIP-seq
☒	☐ Flow cytometry
☒	☐ MRI-based neuroimaging

Animals and other research organisms

Policy information about studies involving animals; ARRIVE guidelines recommended for reporting animal research, and Sex and Gender in Research

Laboratory animals	N/A
Wild animals	N/A
Reporting on sex	N/A
Field-collected samples	N/A
Ethics oversight	N/A

Note that full information on the approval of the study protocol must also be provided in the manuscript.

Dual use research of concern

Policy information about dual use research of concern

Hazards

Could the accidental, deliberate or reckless misuse of agents or technologies generated in the work, or the application of information presented in the manuscript, pose a threat to:

No	Yes
☒	☐ Public health
☒	☐ National security
☐	☒ Crops and/or livestock
☐	☒ Ecosystems
☒	☐ Any other significant area

Hazards: This work involved the generation and growth of GM plants and notably the plant pathogen, Pseudomonas syringae pv. tomato, the latter to alter the effector protein repertoires. All work was carried out under the necessary levels of oversight, authorisation and risk management mandated by the host University and subject to UK legislation. There is no evidence to suggest that the GM plants generated could compete with and/or displace other plants, be more toxic to animals, cause harm to beneficial microroganisms or exhibit altered altered interactions with plant pathogens with adverse effects relative to the equivalent unmodifed plant. Similarly, the genetic modification of Pseudomonas syringae will not alter the ability of any escaping GMO to cause disease in humans.

For examples of agents subject to oversight, see the United States Government Policy for Institutional Oversight of Life Sciences Dual Use Research of Concern.

Experiments of concern

Does the work involve any of these experiments of concern:

No	Yes	
☒	☐	Demonstrate how to render a vaccine ineffective
☒	☐	Confer resistance to therapeutically useful antibiotics or antiviral agents
☒	☐	Enhance the virulence of a pathogen or render a nonpathogen virulent
☒	☐	Increase transmissibility of a pathogen
☒	☐	Alter the host range of a pathogen
☒	☐	Enable evasion of diagnostic/detection modalities
☒	☐	Enable the weaponization of a biological agent or toxin
☒	☐	Any other potentially harmful combination of experiments and agents

Precautions and benefits

Biosecurity precautions	All research undertaken using GMOs is subject to the necessary levels of oversight, authorisation and risk management as prescribed by our University's Genetic Modification and Biosafety Committee and by current UK legislation. Consequently, comprehensive risk assessments are in place which detail potential hazards, inserted genetic material, vectors and risks posed to the environment alongside appropriate control and containment measures, disposal and emergency procedures. Specifically to the use of Pseusomonas syringae DC3000, a non-native UK phytopathogen, the corresponding author Prof Murray Grant, holds a DEFRA license for the use of this pathogen for research purposes and abides by DEFRA-mandated practises to mitigate against accidental or deliberate release.
Biosecurity oversight	See above
Benefits	An increased understanding of plant-pathogen interactions will aid in the development of crops that are more resistent to plant pathogens and help mitigate against the significant current losses in yield both pre- and post-harvest thus impacting future global food security.
Communication benefits	We do not foresee how any harm could result from the publication of this work and therefore publication can only be beneficial (or neutral) to both academics and the wider public.

Plants

Seed stocks	Arabidopsis thaliana reporter lines are available from the corresponding author
Novel plant genotypes	Detailed in Methods section/Origin of transgenic Arabidopsis lines
Authentication	Detailed in Methods section/Origin of transgenic Arabidopsis lines